SALAMANCA CONGLOMERATE

A RECORD OF STORMS, FLOODS, AND TIDES IN DELTAIC-COASTAL DEPOSITS OF THE UPPER DEVONIAN CATTARAUGUS FORMATION

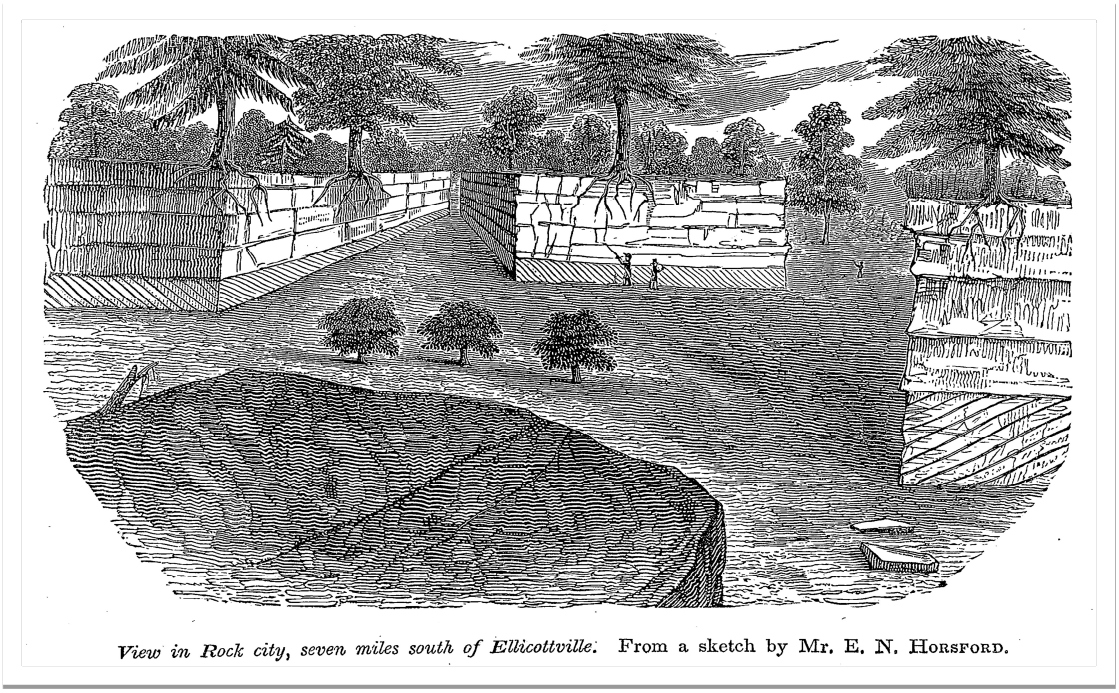

View in Rock city, seven miles south of Ellicottville. From a sketch by Mr. E. N. Horsford.

(Geology of New York, 1843)

JAMES H. CRAFT
Engineering Geologist (retired), New York State Dept. of Environmental Conservation

PREFACE

A version of the following article was prepared after a brief field season for the 2017 New York State Geological Association fall meeting (http://www.nysga-online.net/). Ongoing fieldwork has continued over the last four years and the use of DEMs/GIS has located and correlated Salamanca (and other conglomerates) outcrops over an area of 2000 km^2. The overall interpretation (prograding delta - flood dominated with wave & tide-influence) is the same with some refinements for the type section ("Little Rock City") and near-field areas (Rock City State Forest), chiefly:

- recognition of major channel/bar complexes (up to 5 m thick) interpreted as delta distributaries and tidal channels) overlying marine strata on the western outcrop flank. Also, a large mouth bar was recognized at the base of outcrop #3 as the Rim Trail turns south);

- recognition of pebbly hummocky cross-stratification (HCS coarser than fine sand is uncommon in the rock record). Paleohydraulic estimates of large-scale forms (largest hummock wavelengths > 7 meters; largest pebbles > 5 cm at outcrops # 4 & 5) suggest large waves, combined flows, and energetic storms/hurricanes, in particular, at the top of the sequence.

- recognition of twin conglomerate layers in Allegany State Park separated by 10-15 m of apparent shallow marine strata. The lower unit correlates with the Salamanca and the upper unit is very similar in scale and depositional motif (bi-directional X-strata and HCS) suggesting a re-advance of the paleoshoreline (two Regression-Transgression cycles over ~ 25m-35m formation thickness). Other than the basal Wolf Creek conglomerate, the other historical/locally-named Devonian conglomerates (e.g., Pope Hollow, Tuna Creek, Irish Hollow))appeared to correlate with this pair of Salamanca conglomerates. Other shoaling-upward units are being examined in the Park (largely sandstone, ~ 1-2 m; locations include Sugarbush Cabin loop, Camp Allegany, and Angel Falls).

- recognition of a similar conglomerate of presumed Mississippian age (correlates with Mississippian formations to the east and west and is stratigraphically ~ 100m above the Salamanca in Allegany State Park). Two or three tabular beds of ~ one meter thickness contain abundant coarse-grained HCS with flat pebbles. GIS projection of its caprock plane suggests a much more extensive outcrop of Mississippian rocks in Allegany State Park than currently mapped.

INTRODUCTION

On a hilltop in Rock City State Forest, three miles north of Salamanca, New York, the Salamanca Conglomerate outcrops in spectacular fashion. Part of the Upper Devonian (late Fammenian) Cattaraugus formation, the quartz-pebble conglomerate forms a five to ten-meter high escarpment and topographic bench at ~ 2200 feet elevation amid a mature cherry-maple-oak forest. In places, house-sized blocks have separated from the escarpment along orthogonal

joint sets and variably "crept" downhill. Where concentrated, a maze of blocks and passageways may form so-called "rock cities", an impressive example of which is Little Rock City. The well-cemented blocks permit extraordinary 3-D views of diverse and ubiquitous sedimentary structures and features.

Seven outcrop areas with the most significant exposures were logged over a four-kilometer north-south traverse. The traverse largely follows the east-facing hillside which roughly parallels the presumed paleo-shore of the Devonian Catskill Sea. Extensive "bookend" outcrops at the north face (off the Rim Trail) and at the southeast perimeter ("Little Rock City" along the North Country-Finger Lakes Trail) and vertical (caprock) control allow a nearly continuous look at spatial and temporal changes in sedimentary deposits along a four-kilometer stretch of inferred late Devonian seacoast.

Summary of Findings

Three major depositional environments, reflecting a high-energy and varied coastline, are interpreted from north to south:

Shoreface to foreshore (beach) to channel deposits coarsening-upward sequence - ("north face" **Outcrops #2** from base)

- ~ 2 m of thin-bedded (5-10 cm) wave cross-laminated and small-scale (< 0.5 m) HCS strata; a coset of cross-strata mostly buff, medium sand with some coarse sand, granules, and a few fine pebbles.
- ~ 3 m of amalgamated coarse-grained (1 mm -10 mm) , large (10-20 cm x 50-100 cm) hummocky cross-strata (HCS) interbedded in places w/thin fine-grained (rolling-grain) wave ripples; some trough/planar cross-beds near top.
- ~ 2-m of parallel/low-angle strata of gray interbedded coarse sand and some pebbles.
- ~ 3 m of point bar/lateral accretion/channel deposits.
- pebbly caprock with some hummock forms.

Prograding flood-dominated delta (w/coarse-grained distributaries, mouth bars, tidal channels, bars, and shoals) **(Outcrops # 2, 3, 4, 5, 6 & 7)**

- abundant channels (two main distributaries ≈ 5 m deep, others, ~1-2 m deep) and channel point bars (coarse sand to pebble lateral-accretion deposits of tidal, delta distributary/fluvial channels). Two channel complexes directly overlie fine-grained wave ripple-laminated (marine) sandstones.
- large coarse sand/pebbly hummocky cross-stratification (HCS coarser than fine sand is uncommon in the rock record). Paleohydraulic estimates of large-scale forms (largest hummock wavelengths > 7 meters; largest pebbles > 5 cm at outcrops # 4 & 5) suggest large waves, combined flows, and energetic storms/hurricanes, in particular, at the top of the sequence.
- cross-bedded strata of various dimensions (~ 0.05 m to +1 m), some bidirectional.

- current indicators mainly directed shoreward (E-SE) and alongshore (S) , bi-directional cross-beds common in places; some truncation surfaces show wave influence.
- pebbly caprock with some hummock forms.

Sub-aqueous tidal dune field – **Outcrop area # 7** ("Little Rock City")

- very large scale (up to 5+ m thick) planar 2-D cross-beds with fine-to-coarse sand and abundant granule/fine pebble concentrations and occasional larger pebbles; dune foresets mostly inclined 20-30^{o} and ~ 5-10 cm thick; granule layers usually thicker; some dunes are traceable up to 150 m across several blocks.
- foreset azimuths (50^{o} to 150^{o}) show dunes migrated parallel with and toward the paleoshore with no major reactivation surfaces; most toesets are tangential; planar truncation surface at the top of the dunes shows wave influence.
- a complete 2-3 m dune bedform ("form-set": foreset, topset, stoss preserved); core shows directionally-opposed cross-strata which aggraded vertically until one flow direction (100^{o} – apparent flood tides) prevailed and the ~ 3 m dune began to migrate by periodic foreset deposition.
- $\sim$ 2 – 3 m of point bar/lateral accretion/channel deposits.
- pebbly caprock with hummock forms.

The uppermost sequence of ~ 2-3 m thick channel/lateral accretion deposits with some reddish, well-oxidized strata, plant remains and displays a HCS/wave layer in most places. The caprock varies spatially and is generally similar to the underlying deposits with some reworking evident. Within the deltaic sequence (outcrop #5), the uppermost caprock contains large (average 2-4 cm; up to 7 cm) densely/randomly-packed flat-lying vein-quartz pebbles (and some red and brown sandstone, and red mudstone rip-up clasts not seen elsewhere) with abundant aligned plant remains. The caprock shows a wave ravinement origin with an apparent transgression that brought shallow marine conditions: wave-ripple laminated buff-colored sandstones and an abundant marine fauna not seen elsewhere in the sequence.

The orthoquartzitic Salamanca conglomerate evidently records a high-energy Upper Devonian seacoast, with at least meso-tidal range, as indicated by a pebbly beach, a flood-dominated delta prograding over marine wave-rippled fine sands, very large-scale and very coarse-grained HCS, and a sub-aqueous large-scale dune field formed by strong flood tides. Most of the sequence records delta progradation and sediment transport/redistribution along shore to dunes and beaches by tides and waves and storm circulation of longshore/rip currents in the breaker/surf zone to the shoreface. Well-exposed channel deposits at the top (which overlie wave-truncated dunes and beach deposits at a similar elevation) suggest either expansion of the delta/delta plain or a transition to a coastal plain terrestrial environment (perhaps including a major flood event as suggested by localized large clasts of quartz, sandstone, mud rip-up clasts, and abundant plant fossils) followed by an apparent abrupt rise in relative sea level and a transgression as indicated by subsequent fine-grained wave-formed strata with an abundant marine fossil fauna.

Location and Physiographic Setting

The conglomerate beds of southwestern New York have long been a source of wonder. Appearing in widely-scattered and limited outcrops and more often, as isolated “float” blocks, these beds may more rarely form accumulations of large joint-separated blocks (“buildings”) and passages (“streets”) dubbed “rock cities”. Examples include “Rock City Park” south of Olean (Pennsylvanian age), “Thunder Rocks” (Mississippian? age) atop Allegany State Park, “Panama Rocks” (Upper Devonian age) and “Little Rock City” (the Upper Devonian Salamanca Conglomerate), the subject of this study and perhaps the finest example of a rock city in an unrivaled and freely-accessible setting.

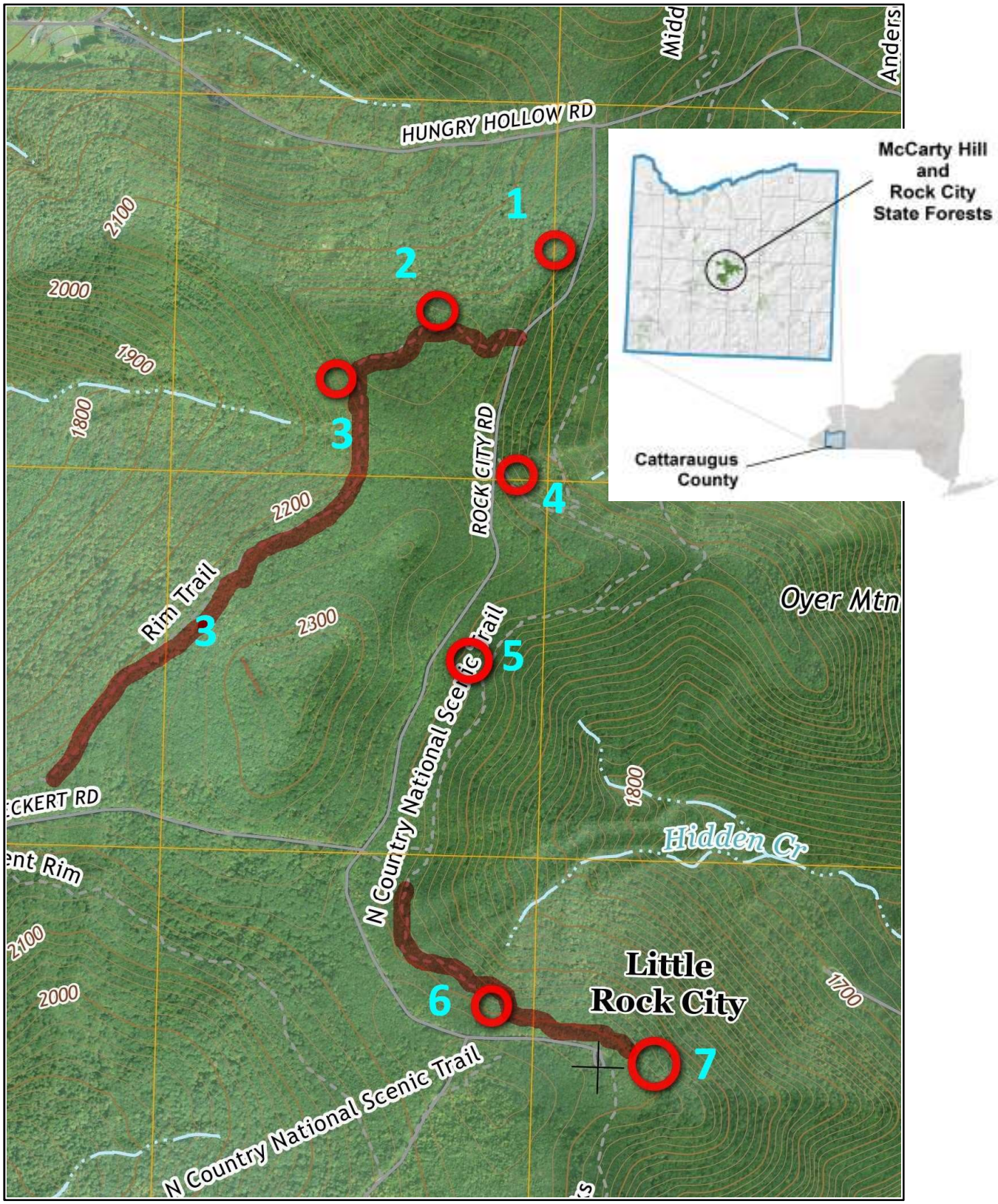

Figure 1. Location Map – Outcrops in Red (#1 - #7)

Scale: 1 cm = 200 m Source: USGS – Salamanca Quadrangle (2016)

The Salamanca Conglomerate outcrops prominently (up to a 10m escarpment) and forms a locally-widespread plateau (~ 2200 feet elevation) in Rock City State Forest and adjacent McCarty Hill State Forest (www.dec.ny.gov/lands/77184.html). This mature forest of cherry, maple, and oak blankets nearly ten square miles of Appalachian Plateau uplands between Ellicottville and Salamanca, NY. "Little Rock City" (LRC - outcrop #7) at the southeast outcrop perimeter is the type locality (Tesmer, 1975). With perhaps the most exquisite exposures, LRC has been an attraction since the early 1800s (e.g., Hall, 1843). Much of the outcrop belt is partially obscured by vegetation, rubble, and in places, glacially-deposited debris but it is readily traceable around the entire hill perimeter as facilitated by a network of hiking trails such as the North Country National Scenic Trail, the Finger Lakes Trail, and the Rim Trail. The outcrop and separated "blocks" are also readily visible with online orthoimagery (https://orthos.dhses.ny.gov/) and with one-meter DEMs (http://gis.ny.gov/elevation/lidar-coverage.htm); the outcrop belt and outcrops of interest can be traced to the Pennsylvania border.

Glaciation – Evidence and Effects

The study area is mapped within the Salamanca Re-entrant, which is part of the unglaciated Appalachian Plateau and northernmost unglaciated area in the eastern United States. Muller (1977) placed an "uncertain" glacier margin at about 1800 feet elevation at roughly one to five kilometers north of the outcrop belt. However, evidence of glaciation in the study area includes: (1) "drab" glacial till layer (chaotically-oriented thin-bedded sandstone in a gray clay matrix) exposed in a small ephemeral stream east of Eckert Road at 2200 feet AMSL; (2) a stretch of outcrops disrupted and largely buried (from outcrop #5 south to Salamanca Road that includes a topographic col/saddle which may have focused ice movement albeit in east-west directions); (3) upside-down garage-sized blocks atop the caprock at outcrop #4 as reported by Smith and Jacobi (2006); and (4) a stretch of tilted strata (point bars at the escarpment appear "pushed" with increased dip in places) at the top of the sequence at outcrop #3 (west Rim trail).

Other areas appear largely unaffected such as the isolated and well-weathered "sentinel" blocks (outcrop #1) and isolated erosional remnants (~ 3m "cubes") perched on pedestals at outcrop #4. It appears then that direct glaciation affected this area variably but periglacial effects such as permafrost, prolonged freeze-thaw cycles, and ice wedging were likely intense. Such conditions likely enhanced block separation, undermining/slump, and downslope movement due to solifluction ("soil flow"/creep due to saturated conditions) and genifluction, (creep in contact with ice/permafrost; e.g., Millar & Nelson, 2001). And the general process of soil creep continues, typically the slowest (~ mm/year on average) but geologically the most significant mass movement process (Allen, 1982).

Structural Features

The regional dip is gently southward (about 30 feet/mile – S/SW; Glenn, 1902 and 20-50 feet/mile – South; Tesmer, 1963). No surface expression of folds or faults were observed but Glenn (1902) reported small folds in Cattaraugus County and the Clarendon-Linden fault complex is nearby in Allegany County (Smith and Jacobi, 2006). Jointing is the most obvious structural feature as it controls the similar block dimensions and the extraordinary rock

exposures on the sides of the blocks. The vertical joint sets are generally orthogonal, spaced ~ 10-20 meters apart, and trend NE-SW (30°-45°) and NW-SE (125°-140°). Per Engelder (1986), the NW-oriented "cross-fold" joints are extension fractures formed by abnormal pore pressures in response to NW-directed tectonic compression during the Alleghanian Orogeny. The orthogonal strike ("release") joints are thought to develop later during regional uplift aligned with NE-oriented residual compressive fabric. The NE strike-joint set may not be as well developed and may waver more in direction and linearity as seen in the gentle sinuous patterns at outcrop #5 and along the "streets" of Little Rock City. Joints can also be affected by changes in lithology and bedding as suggested by the frequent overhangs of the upper channel deposits at the top of the blocks. Apparently these joints either did not readily propagate through the more varied (more permeable?) channel bedding in places or did so at a different spacing and/or direction. Similar effects are can be seen in shale/siltstone/sandstone sequences elsewhere (Engelder, 1986).

Iron Seams

The "iron ore" (hematite) seams of Hall (1843) are red to black in color, 1-3 cm thick, usually sub-horizontal but in places, smoothly contorted and commonly crosscut bedding. The seams appear most common higher in the sequence and in close association with fluvial/deltaic channels/redbeds and plant remains (Fig. 2 - outcrop #1). In the dune field (outcrop #7), iron seams cover several vertical joint surfaces (Fig. 3). And rare cylindrical shapes (10-20 cm in diameter) are suggestive of hollow "logs".

The joint-plane occurrences must have formed during or after joint formation. Jointing involves extension fracturing via abnormal pore pressure generated by tectonic compression (Engelder, 1986). Iron-rich porewater seems possible but the source of large amounts of reduced iron is unknown. However, the high porosity and permeability of this conglomerate could have facilitated later fluid migration. Together with hematite replacement of quartz cement in places, iron seam formation at depth after lithification, and during or after joint formation is indicated.

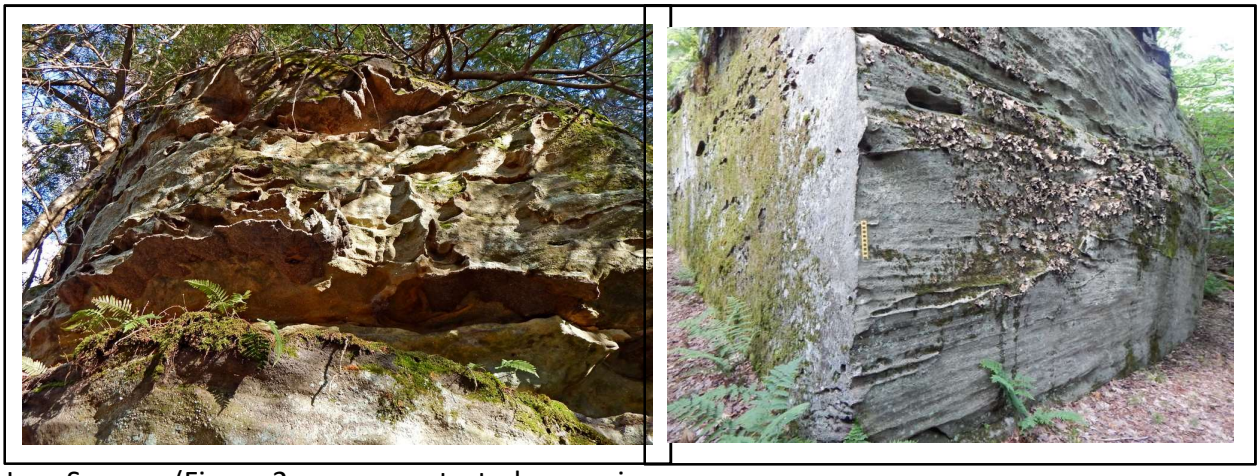

Iron Seams - (Figure 2 - many contorted seams in redbeds. Figure 3 - vertical iron seam on joint plane obscuring large-scale cross-bedding).

In somewhat similar but more varied occurrences in Jurassic sandstones, Chan et al. (2000) reviewed iron mobility and reactions (including Fe-reduction reactions with hydrocarbons) and proposed that mixing of fault-related saline brines with shallow, oxygenated groundwater accounted for the precipitation of iron and manganese. Given the proximity to the world's first oil fields and structural "complications", the mixing of saline brines and hydrocarbons with oxygenated groundwater as well as red bed sources may help explain the Salamanca iron seams.

Previous Work and Stratigraphy

James Hall provided the first scientific descriptions of these rocks ("the conglomerate") as part of the multi-year Geologic Survey of New York (1839-1843). Working in western and central NY (the 4th district), Hall's descriptions and interpretations of some sedimentary structures (e.g., "diagonal lamination" and "ripple marks") and depositional environments (e.g., Medina Sandstone beach) were among the earliest recorded in scientific literature.

Hall's (1843; p. 285-290) conglomerate description (which is difficult to improve upon other than adding "well-rounded" to pebbles) of what at the time was apparently the premier rock city (and perhaps still is) follows below:

> *"The conglomerate consists of a mixture of coarse sand and white quartz pebbles, varying from the size of a pin's head to the diameter of two inches. They are generally oblong, or a flattened egg shape. Some of these are of a rose tint when broken, but white upon the exposed surface. Pebbles of other kinds are very rare in the mass, though red and dark colored jasper are sometimes found.*
>
> *This rock in the Fourth District occurs in outliers of limited extent, capping the summits of the high hills toward the southern margin of the State…From its position, it has been much undermined; and separating into huge blocks, by vertical joints, which are often many feet apart, the places have received the name of ruined cities, Rock city, etc.*
>
> *There are several points in Cattaraugus County where the conglomerate is very well exposed upon the tops of the hills. The best known of these is the "Rock City," about seven miles south of Ellicottville* (present-day Rock City State Forest)*….The sketch* (shown above on the title page) *represents a few of the immense blocks at this place, with the passages between them. The large trees which stand upon the top, have often sent their roots down the sides, where they are sustained in the deep soil, supporting the huge growth above upon an almost barren rock.*
>
> *The masses present the same features as before described, and offer fine exhibitions of the diagonal lamination and contorted seams of iron ore. The rectangular blocks are from thirty to thirty-five feet in thickness, and standing regularly arranged along the line of outcrop, present an imposing appearance, and justify the application of the name it has received."*

The Salamanca Conglomerate is a member of the Cattaraugus Formation of the Upper Devonian (late Fammenian) Conewango Group (Tesmer, 1963, 1975). First described by Hall (1843) as a single widespread unit, "the conglomerate", Carll (1880) named the Salamanca

conglomerate and proposed correlation of several similar beds. Glenn (1902) likewise correlated several conglomerate beds and traced the Wolf Creek conglomerate (a very similar cross-bedded unit of sand and discoidal pebbles overlying "Chemung" beds) and the Salamanca conglomerate from the Portville/Olean area into the Salamanca quadrangle. Clarke (in Glenn, 1902) in a very prescient interpretation, cautioned Glenn about unconformities that rings true today: *"...these sand reefs constantly display indications of deep decapitation due to shifting of bars and change of directions of currents, or a modification by heavy tidal flow on a shelving coast."* Other stratigraphic work (e.g., Caster, 1934) was summarized comprehensively by Tesmer (1975) who concluded that conglomerate correlation is difficult and uncertain due to limited and separated outcrops, glacially-derived cover, probable facies changes, and possible structural complications (e.g., slight dip changes/folding/faulting). Tesmer (1975) tentatively placed the Salamanca member in the middle of the Cattaraugus formation, following Glenn (1902) who had mapped the Salamanca member well above (~ 60-70 m) the basal Wolf Creek member in the Olean area.

Baird and Lash (1990) noted some progress with correlation of the Panama Conglomerate member with the LeBeouf Sandstone in Chatauqua County and also noted the need to locate and observe the upper and lower contacts of these conglomerate units in order to place them in geological context (this study offers glimpses). Smith and Jacobi (2006) placed the Salamanca conglomerate at the base of the Conewango Group which appears to place it between the Wolf Creek conglomerate (type section near Olean, NY) and the westernmost Panama conglomerate (type section at Panama, NY).

PALEOGEOGRAPHY - GEOLOGIC SETTING

A paleolatitude of 25-30 degrees south (Fig.4) and a warm, seasonally wet-dry climate has been posited for the Upper Devonian of New York (e.g., Woodrow et al., 1973; Scotese, 2000). Southeast trade winds likely prevailed but the Acadian highlands presented a rain shadow (Woodrow, 1985). However, abundant rainfall would be expected from postulated monsoonal circulation (Witzke, 1990, Streel et al., 2000, Smith and Jacobi, 2006), perhaps similar to the present-day Indian Ocean/Indian subcontinent or the northern coast of Australia. The Arafura Sea and northern Australia coast, with frequent tropical cyclones and a wet-dry monsoonal climate, is considered a modern analog for the epeiric Catskill sea and coast (Dott and Batten, 1980; Woodrow 1985). Climate is a primary control on source-to-basin sediment flux and in warm climates, siliciclastic flux is greatest under highly seasonal rainfall (Cecil, 1990).

Given the likelihood of monsoonal rainfall, frequent floods, episodic hurricanes (Duke, 1985; Craft and Bridge, 1987; Baird and Lash, 1990; Smith and Jacobi, 2006) with possible storm-flood (Collins et al., 2016) and storm-tide coupling, and evolving plants which paradoxically may have increased weathering rates in places (Berner, 1997), significant weathering and transport of sediment to the Catskill Sea would be expected. In addition, pulsed orogenesis in the source area (the third collisional tectophase of the Acadian Orogeny; Ettensohn, 1985) would likely have acted to increase stream/erosional gradients significant fluxes of sediment into the basin, and basin subsidence in response to tectonic/sediment loading on the crust.

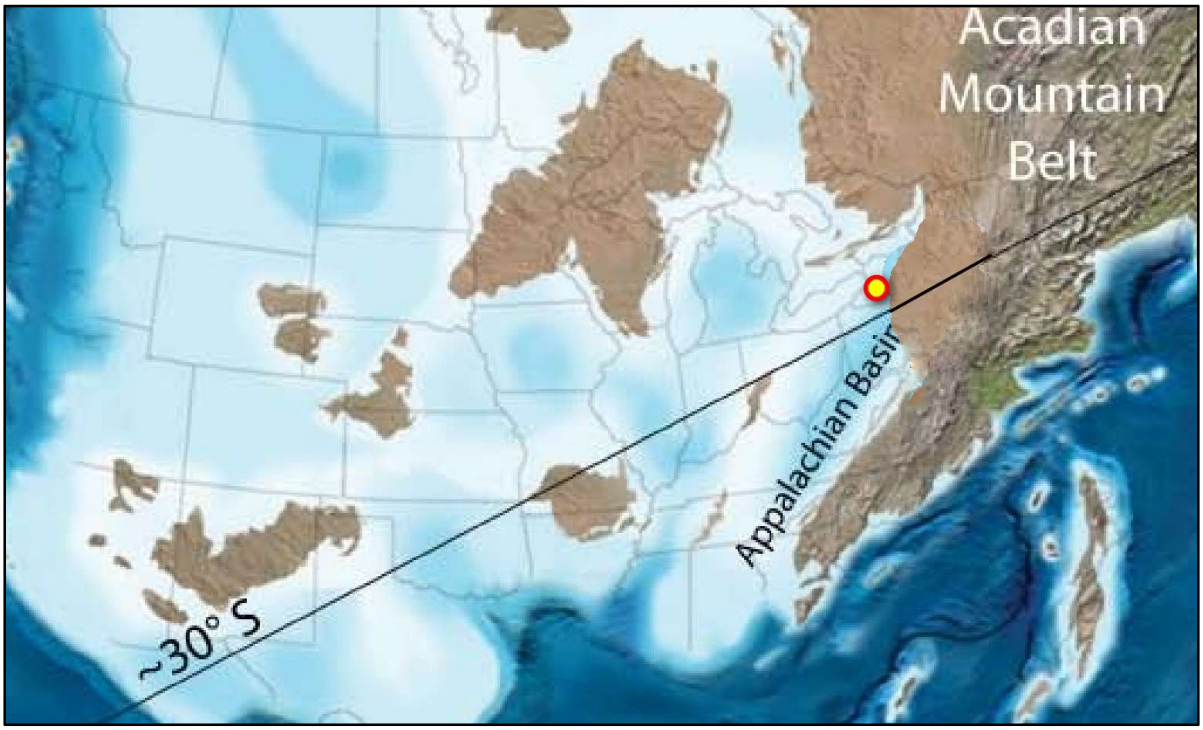

Figure 4. Late Devonian paleogeographic map – study area highlighted (modified from Blakey, 2017

and Zambito, 2011; shoreline extended into western NY; all boundaries approximate)

Basin Subsidence/Deposition Rates

The average subsidence rate in the Catskill foreland basin was nearly an order of magnitude higher in the upper Devonian than the middle Devonian (Faill, 1985) with deposits as thick as ~ 2000-3000 m over the ~ 14 million year duration of the Upper Devonian. In western New York, Faill (1985; Fig. 7) showed an estimated subsidence/deposition rate of ~ 100 m/million years (or roughly 2 million years to deposit the ~200 m Cattaraugus Formation). Coupling that rate with an average shoreline advance of ~ 30 km/million years (Dennison, 1985; Fig. 4), gives a rough volumetric deposition rate of three million cubic meters per million years per linear meter of prograding shoreline.

Shoreline

The coastal zone of the Devonian Catskill Sea varied in space and time as shown by the varied interpretations of shoreline deposits. Coastal paleoenvironments included deltas, distributary channels/mouth bars, tidal channels/flats, mud flats, and beaches (e.g., compilation in Sevon, 1985). Despite a number of early tidal interpretations, an assumption persisted that the probable tidal range/energy was low. But seminal work such as Johnson and Friedman (1969; tidal channels/flats) and Rahmanian (1979; tide-dominated delta) and tidal modeling by Slingerland (1986) and Ericksen et al. (1990) which suggested at least mesotidal (2 m - 4 m) range, recognition of tidal coastal deposits increased over time (e.g., Bridge and Droser, 1985; Bridge and Willis, 1988; Bishuk et al., 1991, 2003; Duke at al., 1991; Willis & Bridge, 1994; Prave et al., 1996).

Slingerland and Loule (1988) documented a tide-dominated shoreline (tidal channels / flats / shoals / estuaries) with a wave-dominated (sand ridges) offshore in a shore-parallel, time-equivalent (mid-Frasnian) transect through central Pennsylvania. They posited that nearshore circulation was to the SW (clockwise), estimated tidal range was high meso-tidal, and that three major clastic dispersal systems (drainage basins) existed across Pennsylvania. They also noted that meandering fluvial deposits capped all sections studied and that a lack of mouth bars and levees was attributed to strong tidal currents.

In a review of Devonian Catskill alluvial and coastal deposits, Bridge (2000) noted several coastal features in common: *"(1) sandy, tide-influenced channels; (2) shallow bays and tidal flats where mud and sand were deposited; (3) rarity of beaches; (4) storm-wave domination of the marine shelf. Much of the variability in the deposits across the area could be explained within the context of a wave- and tide-influenced deltaic coastline with a tidal range that varied in time and space."*

Regarding variations in tidal ranges, Reynaud and Dalrymple (2012) noted that since tides interact strongly with shelf and coastline morphology, changes in relative sea level can have a profound effect on tidal currents and deposits. Tidal resonance (amplitude strength) varies with shelf width (i.e., highest at increments of one-quarter of the tidal wavelength) and is directly affected by changing sea levels. They stated that: *"The increase in tidal influence can be geologically instantaneous in situations where the geomorphology changes rapidly. This was the case in the Gulf of Maine-Bay of Fundy system, which changed from microtidal to extreme macrotidal over a period on only a few thousand years."* Short-term changes then (e.g., tectonic or climate-driven sea-level variations) can bring about rapid change, *"potentially causing an alternation between tidal and non-tidal deposits" and "different parts of the transgressing sea can become resonant at different times"*. Also, once tidal resonance has been reached, further increases in sea level often result in a decrease in tidal influence. They suggested, as possible examples, abandoned tidal dune fields preserved beneath North Sea muds and tidal sandbodies in the Devonian Castkill Sea. They cited Ericksen et al. (1990) for the latter, who did not provide specific examples but the Salamanca tidal dune field at LRC is a possible example of decreasing tidal influence with wave-truncated dune tops overlain by channel deposits.

<u>Sediment Sources & Dispersal Systems</u>

Based on the inferred position of the Acadian orogen (Faill, 1985), source areas were likely located about 400 km to the southeast (cf. Pelletier, 1958) during Fammenian time. Weathering and erosion of actively-rising mountains produced detritus (including tabular vein quartz gravel) that was conveyed by streams to the foreland basin. As the shoreline advanced, drainage networks continually expanded and likely interacted to varying degrees. Sevon (1985) depicted up to six "sediment dispersal systems" which could have affected western NY, Slingerland and Loule (1988) noted three major drainage systems, and Boswell and Donaldson (1988) posited five stable drainage systems with large trunk streams for the Fammenian of West Virginia. The size of these drainage basins and streams are difficult to gauge but given an alluvial plain of at most 400 km, these were not the large continental rivers and deltas of today. Bridge (2000) noted that Catskill river channels were smaller near the coast (i.e., sinuous,

single-channel rivers, tens of meters wide, maximum depths of 4 - 5 m, sinuosity of 1.1-1.3, mean bank-full flow velocity of 0.4 - 0.7 m/s) and perhaps distributive (delta-related). With increasing distance from the coast, slopes increased, rivers became wider (up to hundreds of meters), deeper (up to 15 m), coarser grained, and possibly braided. In this study, two large channels were identified along outcrop #3, one associated with a mouth bar complex and the other about 600 m south on the Rim Trail. Based on point bar deposits, a channel depth of 5 meters was inferred for both paleo-streams. And given their proximity and progradation over marine deposits, these paleo-streams can be considered distributaries.

Sediment - Sand & Pebbles

Other than localized rip-up clasts, no mud-sized sediment was observed. Quartz sand ranges in size from fine to very coarse, is sub-rounded to sub-angular, and composed largely of clear monocrystalline quartz. Clear quartz is mainly derived from intrusive plutonic rocks such as granite; such crystals are generally < 1 mm and are the source of most quartz sand. Cloudy polycrystalline quartz (the stuff of pebbles) predominates in coarser (1-2 mm) grains. Sand lithology is +95% quartz with occasional opaque grains including magnetite. Fine-grained magnetite comprises a very minor overall component (<<1%) of sand but it may concentrate locally along laminations in places. Bagged samples of disaggregated sand obtained from nearshore marine, beach transition, and channel deposits were magnetically-separated; all showed trace amounts of magnetite with channel deposits containing somewhat higher amounts. Since the specific gravity of magnetite (5.18 g/cm^3) is nearly double that of quartz, fine (0.125-0.25 mm) grained magnetite sand is roughly the hydraulic equivalent of medium (0.25-0.5 mm) quartz sand. At the shoreface/foreshore transition and in foresets of some dunes, dark-colored laminations and streaks occur. However, where samples could be obtained (e.g., moss-weathered outcrops), magnetite was rare. Magnetic separation showed partial black coatings on quartz grains and separated black flakes (magnetic attraction varied but mostly slight; possible hematite?).

Medium to very coarse sand dominates much of the sequence with variable percentages of pebbles; where interbedded with single or multiple layers of discoidal pebbles, the pebbles usually conform to bedding and accentuate sedimentary structures.

PEBBLES

Perhaps the most interesting geological feature of the Salamanca conglomerate (in addition to cross-bedded monoliths the size of houses) are the ubiquitous, well-rounded, discoidal, vein-quartz pebbles. The Salamanca is classified as an orthoquartitic conglomerate since the pebbles are lithologically and texturally mature. The milky polycrystalline quartz pebbles range from ~ 2 mm to 60+ mm (very fine to very coarse pebbles), average ~ 8-10 mm in size and are oblate ("flattened") ellipsoids in shape. Pebble lithologies are +98% quartz with minor amounts of red jasper and rock fragments. Shallow pits and fracture traces are evident on the surface of many, mainly larger, pebbles. Most pitting is likely related to point-contact pressure solution upon burial which probably provided much dissolved silica for this well-cemented unit. Some surface ornamentation may be impact-related such as possible percussion marks on beach

clasts (Allen, 1970) and V-shaped pits. The milky/cloudy nature of the polycrystalline quartz pebbles derives from microscopic fluid inclusions which disperse light. Fluid inclusions are consistent with a hydrothermal origin where silica-rich fluids were likely emplaced under pressure and crystallized rapidly in fractures of an active orogen source zone. And sedimentary deposits of vein quartz, such as channel bars/floodplains and bedrock in the drainage basin, may also provide source material.

Pebbles often conform with and accentuate sandy stratification and hence are very helpful in defining sedimentary structures and paleoflow directions, and assessing paleohydraulics. However, in beds where pebbles dominate (e.g., minor sand matrix, clast-supported,"open framework gravels" such as present in channel fills, bars, and storm beds), stratification may be crudely developed and difficult to interpret. Pebble imbrication can be helpful such as the common orientation of oblong pebbles transverse to flow but pebble inclination may be ambiguous. Jumbled/chaotic/unstable pebble orientations suggests disequilibrium in rapidly depositing or changing flows (e.g., an "unsteady" combined flow of tides and waves).

Pebble Shape/Origin

The origin of the distinctive discoidal pebble shape has been ascribed to beach abrasion since the Salamanca was named (Carll, 1880) and accepted over time by Glenn, 1902, Tesmer, 1975, and Miller, 1974, as cited by Baird and Lash 1990). While appealing, it is not clear how an entire population (trillions?) of extremely durable quartz pebbles could be systematically and symmetrically abraded/flattened to yield co-planar sides and with a probable concomitant mass loss of 70 to 80% (assuming a quasi-spherical start and an ellipsoid finish with a "c-axis" shortened by 75%). Prolonged abrasion experiments show little mass loss for quartz pebbles after initial edge rounding (e.g., Krumbein, 1941; Keunen, 1956; Attal and Lave, 2009; Domokos, 2012). Also, at this locality the majority of Salamanca pebbles are found in channel deposits; beach deposits are not common. It seems clear then that the cloudy pebbles of vein-quartz derived their tabular shape from their origin in tabular quartz-filled fractures (veins) in the source area and rounding/smoothing during stream transport. As Pettijohn (1975) noted, the end-shape of sedimentary quartz is an expression of its initial shape.

Pebble Dimensions - Fractures/Fragmentation

Clast thickness is largely determined by the dimensions of tabular quartz veins in the source area. Caliper triaxial measurements of ~ 100 pebbles spanning the available size range yielded a C-axis (the short ellipsoidal axis) range of 1.5 mm to 16 mm which suggests veins of that size range in the source area. And that rather restricted thickness range suggests a rather consistent source area of narrow tabular veins of quartz (few "rogue" spheroidal clasts; other lithologies are less durable). And hydraulic (size) sorting and fracturing during extended fluvial transport would tend to limit clast size (the majority of pebbles are < 20 mm). Larger clasts then are sequentially sorted out; Pelletier (1958) showed an exponential decline in pebble sizes with distance from the source area in the Pocono Group. The sudden appearance of some very coarse pebbles (up to 60 mm and 25% different lithologies; sandstone, metamorphic, and mudstone clasts) at the top of the caprock suggests an unusual event or process.

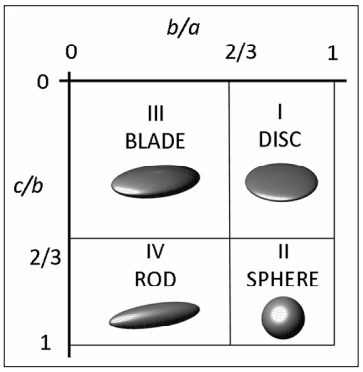

Figure 5 – Zingg diagram

Figure 6 -Well-rounded quartz pebbles (~ 2mm to 60 mm)

However, smaller size ranges (< 8 mm) trend toward, and in particular, many 2-4 mm ("granules") pebbles, plot within the Sphere zone. The C-axes, while thin (1.5 mm – 3 mm), are still recognizable as parallel which suggests the same vein origin. These more equant shapes result when the A - B axes approach the C-axis in dimension.

So the C-axis is essentially fixed (vein-pebble thickness = lowest common diameter); the A and B axes can get smaller due to breakage normal to C. The suggested mechanism is the greater susceptibility of thinner veins and clasts to weathering and fragmentation at the outcrop and in early transport in high-gradient streams. Fracture traces, often outlined by iron-oxide staining, are common and are generally normal to the two co-planar sides (A & B axes). Some pebbles show smoothing/rounding of fracture-parallel edges (missing chunks) which suggests fragmentation/smoothing occurred during transport (Fig. 6). Other pebbles show sharp-edged breaks which, if natural, suggest little transport after fragmentation. So planes of weakness would tend to focus breakage along the short "C" axis and the thinner the veins/pebbles, the higher the expected rate of disintegration (lots of thin veins/pebbles = lots of milky granules and odd shapes, e.g, irregular or roughly triangular, appear more common in small pebbles). The highest fragmentation rates during transport would be expected in near-source high-gradient streams where strong flows, a wide size range of particles in motion, and high impact velocities which, along with existing planes of weakness, would promote fragmentation (e.g., Attal and Lave, 2009).

<u>Rounding</u>

Experiments have shown that lithology controls abrasion rates (e.g., Keunen, 1956, Domokos et al., 2014). Quartz pebbles are extremely durable with fairly rapid rounding (Attal and Lave, 2009; Domokos et al, 2012) but little overall change in clast diameter ("virtually indestructible", Pettijohn, 1975; Southard, 2006). In an elegant series of experiments, modeling, and field studies (Domokos et al,. 2012; Miller et al. 2014) demonstrated that *"abrasion occurs in two well-separated phases: first, pebble edges rapidly round without any change in axis dimensions*

until the shape becomes entirely convex; and second, axis dimensions are then slowly reduced while the particle remains convex." The first phase occurs mainly in high-gradient, source-proximal streams, the second, in lower-gradient alluvial plains where size sorting due to stream hydraulics and lithologically-controlled abrasion prevails." Coupled with the fragmentation process noted above, most sizing and shaping (fragmentation) and rounding (convex shaping) of pebbles likely occurs in near-source high-gradient streams whereas most hydraulic (size) sorting and abrasion (slight for quartz) occurs in lower gradient alluvial plain streams. And considering "chipping", which contributes smaller particles to the bed-load, clast attrition by bed-load transport can occur by abrasion, chipping, and fragmentation. But clasts < 10 mm generally only abrade; chipping and fragmentation require sufficient clast mass and momentum to collide effectively. (Novák-Szabó et al., 2018; Miller and Jerolmack, 2021).

The Granule "Problem"

Pettijohn (1975) and Southard (2006) noted a general scarcity of very coarse quartz sand and granules (1 mm - 4 mm) in the rock record. The cause appears related to the fact that the most common sizes of quartz crystals in plutonic rocks, the source of most quartz sand, are mostly less than one-millimeter. The Salamanca and other Upper Devonian conglomerates have an abundance of coarse sand, granules, and fine pebbles likely produced by fragmentation and chipping of vein quartz particles during fluvial transport. These size ranges are more spherical than larger pebbles and readily transported by nearshore currents and are abundant in dunes and nearshore marine deposits. The general source of quartz grains can be roughly distinguished in field: Clear = monocrystalline plutonic sources vs. Milky = polycrystalline vein sources. The tannish granule/pebble layers ("grain striping") within the light gray sands of large dune foresets is a macro-example.

Possible Vein-Quartz Source-Area Analogues

Pettijohn (1975) and Baird and Lash (1990) noted that large vein quartz accumulations imply the destruction of large volumes of source rocks since quartz veins make up a just small percentage of normal lithosphere. However, vast amounts of vein-quartz pebbles transported within fairly limited drainage basins for tens of thousands of years suggest an unusual lithosphere (an abundance of quartz veins) within areally-limited drainage basins/source areas. Hack's (1957) law indicates that a stream about 400 km long (approximate distance from late Devonian shoreline to the Acadian orogen) would have a drainage basin of roughly 20,000 km^2. The near-source catchment width is uncertain but probably on the order of 100 km. Whereas clasts of various sizes would be expected to "banked" within an immature drainage network (e.g., at near-source alluvial fans, "wedge-top depozones", and with sorting downstream, in fluvial bars and channel deposits, and possibly older formations), a relatively small catchment area suggests a large concentration of quartz veins in a limited source area. And a much more extensive sedimentation pattern of conglomeratic, largely fluvial, deposition continued in the Mississippian/Pennsylvanian Periods. Deposited largely in Pennsylvania, the larger, more equant quartz pebbles of the Olean/Pocono/Pottsville formations suggest unroofing of vast quantities of thicker quartz veins.

Possible analogues for a vein-quartz source terrain include the Ouachita Mountains where more than 8000 meters of Paleozoic strata were folded during the Mid-Pennsylvanian Ouachita

Orogeny. Innumerable steeply-dipping fractures, related to the major folds and faults of the region, controlled the emplacement of hydrothermal quartz (Miser, 1943; Engel, 1951). And the famous Witwatersrand gold deposit in South Africa (source of 50% of the world's gold for over a century) is a Precambrian fluvial conglomerate with discoidal vein quartz (~ 30 mm) pebbles that has received much study. Another example of an abundant source area of vein-quartz as well as long distance transport of discoidal pebbles is the Miocene uplift in the southern Appalachians. As reported by Missiner and Maliva (2017), pulsed tectonism resulted in a surge in coarse siliciclastic sediment (including abundant discoidal vein-quartz pebbles of up to 40 mm in diameter) and long distance (up to 1000 km) fluvial transport.

Fossils

Plant remains are common in channel and associated deposits particularly within the deltaic sequence. With the exception of possible escape burrows in a channel base, trace and body fossils were not observed within the Salamanca conglomerate. However, abruptly overlying the caprock are finer-grained buff sandstones that contain an abundant brachiopod fauna and rich marine faunas are common in shallow marine deposits nearby. For example, an intact *Productella sp*. was found lying directly on the caprock seemingly in life position (Fig. 24).

Hall (1843) noted that fossils are extremely rare within the "conglomerate" citing 3 brachipod species in a sandy correlative of the Panama member. Tesmer (1975), citing the work of Butts (in Glenn, 1902) in the nearby Olean quadrangle, noted two brachiopod species in the Salamanca, Camarotoechia contracta and Crytosprifer sp? along with 13 pelecypod species, an ammoniod, and a gastropod.

DESCRIPTION OF LITHOFACIES

Three major categories of sedimentary structures observed in the Salamanca Conglomerate are:

- Structures formed mainly by wave (oscillatory) currents - Coarse-grained hummocky cross-stratification (HCS) and wave ripple cross-stratification, and low-angle planar beds (foreshore);
- Structures formed by unidirectional currents - 2-D and 3-D cross-stratification (2-D planar [mostly] and trough cross-beds of various scales (0.05 to 5 m) and low-angle to planar strata (bedload sheets);
- Large-scale structures (macroforms) formed by fluvial and tidal processes - Low-angle stratasets ("point" bars), channel-forms/fills, mid-channel bars, stacked/downlapped sigmoidal strata sets (components of mouth bars).

Given the diversity and overlap of these structures and processes, each will be described and interpreted separately followed by a synthesis of the depositional environments.

The overall formation geometry is tabular, ranging up to 10 m thick with major bedding planes of one to two meters thick. With a pebbly caprock of 10-50 cm in thickness, the well-cemented conglomerate of coarse sand and pebbles forms a prominent topographic bench (i.e, the Appalachian Plateau) locally and the base shows little relief where rarely exposed. Channel-forms, associated low-angle stratasets, and mouth bars outcrop prominently along the well-exposed northern and western rims (outcrops #2 - 3). comprise a thin (2-5 m) channel belt.

Wave Ripples - Rolling Grain to Vortex to Hummocks

Wave ripples may be symmetrical as formed by orbital wave oscillations or asymmetrical to varying degrees as formed by combined (oscillatory and unidirectional) flows. Larger forms in particular may require a net influx of sediment via transport by unidirectional currents. A continuum of ripple wavelengths was observed ranging from 0.05 m to > 10 m. 2-D vortex ripples are uncommon whereas 3-D forms are abundant and may be considered small-scale hummock/HCS (range up to ~ 0.5 m). Larger 3-D hummocky ripples form HCS and range from ~ 0.25 m to > 10 m. Both 2-D vortex and smaller-scale 3-D HCS transition laterally and vertically into larger HCS.

Rolling-grain ripples may form as sediment begins to move under waves. Near-bed wave oscillations set up low-profile, symmetric, sediment furrows spaced by a relation of the orbital diameter. As the orbital velocity increases, the ripples may grow vertically and develop flow separations at the crest, thus becoming vortex ripples. Rolling-grain ripples were observed at the top of some gravelly amalgamated HCS beds at outcrop #2. The very thin (~ 0.005 m), buff-colored layers that may weather in relief and help distinguish the HCS beds. The base of outcrop #6 also includes some examples.

Vortex wave ripples range from 0.05 m to 0.5 m in length and average 0.05 m to 0.1 m in height. With linear, sharp to rounded crestlines and symmetric to asymmetric trochcoidal profiles, wave-ripple cross-laminations may display discordant and/or concordant laminae with common truncations and a wavy base. Usually a thin-bedded medium sandstone with a sugary somewhat friable texture and gray-green color, amalgamation is common as are lateral transitions to HCS (e.g., outcrop #5 and the base of outcrop #6 (Fig). With increasing orbital velocities, 2-D ripples become less steep, rounded over and transform into 3-D ripples (Southard et al., 1990) and increase in size with increasing orbital velocity (Pedocchi and Garcia, 2009). With a combined flow, even a small component of unidirectional current can lead to rounded profiles, ripple asymmetry and migration (Dumas et al., 2005).

Hummocky cross-stratification (HCS) was first described by Gilbert (1899; "giant wave ripples", see highlighted section below), was "re-discovered" by Campbell (1966; "truncated wave-ripple laminae") and then formally described and named "hummocky cross-stratification" by Harms et al. (1975). The typical criteria are:

- low-profile 3-D domal bedforms ("hummocks" with wavelengths of one to a few meters by ~ 0.5 m high separated by "swales"; usually within a tabular bed);
- internally stratified by gently-dipping (<15^{o}) convex laminae with no preferred orientation which typically thicken toward the swales and thin toward the hummock;
- composed of coarse silt to fine sand which may be form-concordant (isotropic form) and/or exhibit low-angle truncations (anisotropic form); and

- the bases may be erosional or conform to the strata below. Sole marks are common where interbedded with shale and planar laminations may occur above the base followed by HCS.

  A related type of cross-strata consisting predominately of concave-upward laminations ("swales") about 0.5 m - 2 m wide and a few decimeters deep is termed "swaley cross-stratification" (SCS; Leckie and Walker, 1982). It occurs mainly above HCS in coarsening-upward sequences.

Hummocky cross-strata observed within the Salamanca Conglomerate display typical hummocky forms and strata but with significant differences:

Larger grain sizes - Mean grain sizes of 1 mm - 2 mm (very coarse sand) are an order of magnitude greater than typical fine-grained HCS and "flat" pebbles (2 mm to > 20 mm) commonly follow stratification. Some very coarse-grained, large dimension HCS display some inverse grading with large pebbles at or near the top of the bedforms (see Fig.). One notable example is nearly all clast-supported pebbles and crudely stratified on the flanks but with chaotic fabric (even vertical clasts) at the center (Fig.)..

Note: Reports of coarse-grained HCS are uncommon in the literature and conglomeratic HCS, quite rare. Brenchley and Newall (1982) described HCS in coarse-grained sandstones. DeCelles and Cavazza (1992) recorded HCS of up to coarse sand size that was deposited in shallow (2-5m) depths. McClung et al. (2016) reported conglomeratic HCS in Fammenian-aged strata in West Virginia but the gravels appear in lag deposits and cross-bedding beneath the finer-grained HCS. And Jelby (2020) noted a variety of HCS types including "complex" gravelly forms from the Cretaceous of Svalbard.

.

Figure 7. Typical HCS on left; Conglomeratic HCS on right

Left: A fine example of fine-grained HCS "float"ing on a hillside in Allegany State Park. Note the domal 1.5 m bedform with concordant laminations that arch gently in all directions, thin upward, and are capped by small (~10 cm; likely anorbital) wave ripples that bend/refract around the hummock (likely as the storm waned). This location is about 50 m below the Salamanca outcrop in the park.

Right: Very large/coarse HCS at outcrop #5 in RCSF (tape ~ 50 cm). Note low-angle strata defined by discoidal pebbles, some in excess of 2 cm in diameter. About half of the hummock is

shown extending 3.5 m in one direction. This and some other large examples exhibit poor sorting with general coarsening upward/inverse grading with some of the largest pebbles at or near the top of the bed. Bedload and suspended transport by a combined flow is indicated: intense oscillatory currents (to mobilize the sediment and mold the bedforms) and unidirectional currents to transport it.

Below: Full length view of hummock above; crest is part of the caprock (total L = 7 m; tape = 1 m)

Above: Outcrop #5 – Two views (1.5 m vertical exposure) / same channel & x-beds - Large (rip?) channel(s)/gutter(s) on left; large-scale (0.5 m) cross-beds oriented south (longshore direction) and hummocks in pebbly caprock.

Below: Very large amalgamated HCS at the top of the sequence, SW of LRC

Amalgamated HCS (outcrop #5) - Largest and coarsest at top (notebook = 20 cm); bases show both scour and drape; small-scale HCS present at base of upper HCS on left. On right, subjacent to caprock, note 3-D view of hummock at tape (= 1 m) and similar hummock to the left in same bed. Finely-laminated wave ripples (med. sandstone) just below major beddding plane.

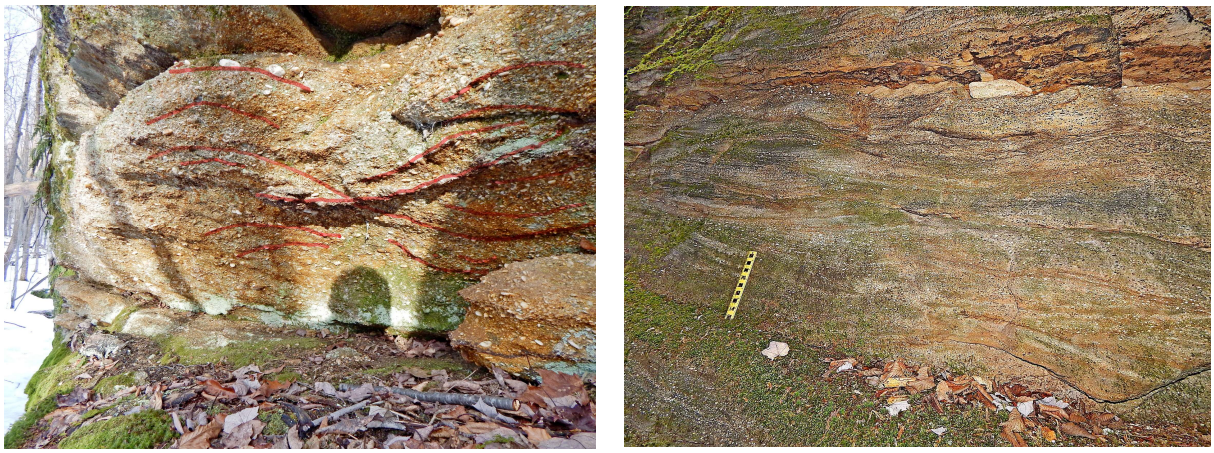

Above: Outcrop #4 – very coarse clast-supported HCS Outcrop #2- Granule HCS ; ruler = 18 cm.

Hummock wavelengths – Mean wavelength ≈ 2 m (see Fig. 11); based on 53 "apparent " hummock measurements in outcrop cross-sections and block corners (hence likely biased low) and commonly exceed 5 m. The uppermost stratum just below the caprock appears to contain the largest examples and are best exposed at outcrops #4 and #5 where the coarsest (up to 6 cm) caprock clasts were observed. (Figs. 7 , 8). And at the lower range, smaller-scale forms of about => 0.25 m and includes some pebbly (clast-supported) examples (e.g., small "domes" ~ 0.30 m) beneath larger forms at outcrop #2. Also, the caprock at outcrops #2 and 7 show domal bedforms at this scale. Campbell (1966), Dott and Bourgeois (1982), and Craft and Bridge (1987) reported similar low-end ranges.

Bedding dip angles – As shown in Fig. 8 , dip angles calculated from hummock height and ½ length (arcsin H/(L/2)) for 53 hummock measurements yielded a range of 43° to 7° degrees with a distinct inflection point at about 20 degrees. Of the 15 hummocks with laminae dips > 20°, 11 hummocks are < 0.5 m in length. Kriesa (1981) and Craft and Bridge (1987) also reported higher dips (~ 25°) for smaller-scale HCS.

Figure 8. Outcrop #5 - Big HCS - (L > 10 m; H ≈ 1 m)

Big pebbles – caprock; 18 cm ruler

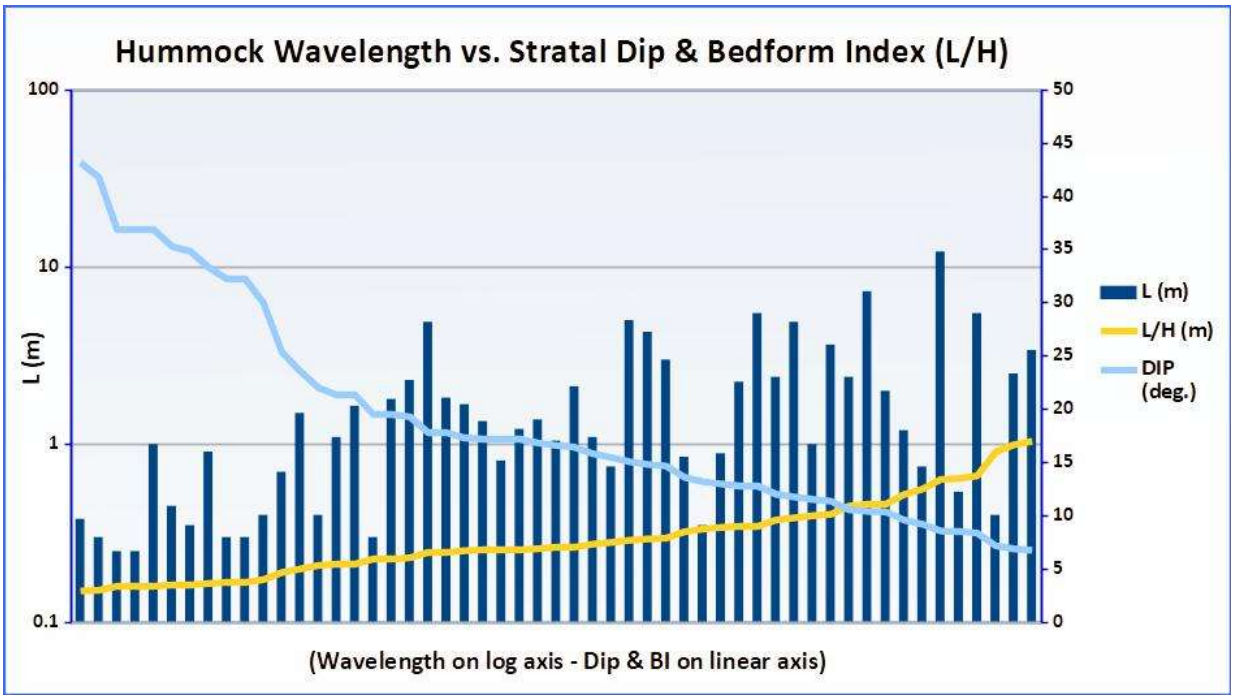

Figure 9. Smaller hummocks tend to show higher dips perhaps the consequence of a 2D-3D bedform transition and a non-equilibrium bed state. Similarly, these forms show a low bedform index (BI) due to a "taller" profile. The overall BI is < 15 and mostly < 10 as is characteristic of wave ripples (unidirectional dunes show a BI range of about 15 - 40; Leeder, 2009). Trends in these parameters (and a symmetry index) may help identify distinct combined-flow bedforms.

Unidirectional cross-beds of variable foreset inclinations (range of about 20 - 30°) are interspersed in places with HCS. Most are less than 0.3 m in thickness, up to 10 m long, and directed generally southward (roughly shore-parallel). At outcrop #5, two cross-beds of about 5 to 10 meters in extent appear to grade into HCS although the exposure is poor. Amalgamation is common and on display at outcrops #2 and #5 (Fig. 7.).

Figure 10. Plot of measured hummock dimensions shows a strong linear trend indicating similar form with size and a continuum of orbital 3-D wave ripples (hummocks). Also, pebble size, where present, typically scales with hummock size corroborating larger flow velocity/wave-forcing.

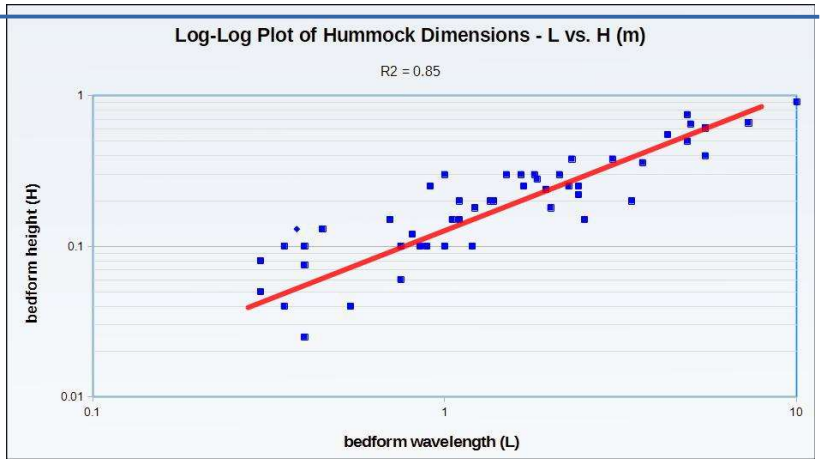

Considered a signature of storm wave deposition, HCS has been reported in numerous studies of shallow marine and a few lacustrine deposits, ancient and modern, and in laboratory flume

experiments. Experiments have established the overall hydraulic conditions and sediment properties necessary to form wave ripples of various scales, in particular, HCS (a.k.a. large wave ripples). Key lab studies include Southard et al. (1990), Arnott and Southard (1990), Dumas and Arnott (2006), Cummings et al. (2009), Pedocchi and Garcia (2009), Perillo et al., (2014, and Ruessink et al. (2015).

Perillo et al. (2014) and others have demonstrated a continuum of wave ripples of increasing size under oscillatory (wave only) and combined flows with wave dominance. Given these and other results, direct field observations (Greenwood and Sherman, 1986 ; Amos et al., 1996; Keen et al., 2012), and compelling evidence of sediment transport from the rock record, a wave-dominated combined-flow origin is evident for most HCS.

Most lab work focused on fine-grained sediment since the vast majority of ancient wave deposits are fine-grained and coarser sand can present equipment limitations. In a wave tunnel study with fine and coarse sands, Cummings et al. (2009) reported large wave ripples (LWRs; wavelengths 50–350 cm, heights 10–25 cm) that varied with grain size. Fine-grained LWRs were subdued, 2-D (sharp-crested) or 3-D (smooth-crested) that resembled HCS. Coarse-grained LWRs were of 2-D form with linear crests and steep ripple faces as reported in some ancient deposits (e.g., Leckie, 1988, who posited that such 2-D ripples are the coarse-grained equivalent of HCS). In addition, they noted that all LWRs were orbital and that the wavelengths of fine-grained LWRs scaled on average to $0.6d_o$, which is close to $0.65d_o$, the most commonly reported scaling ratio for orbital ripples starting with Komar (1974). By contrast, coarse-grained LWRs scaled on average to **$0.4d_o$**. ; similar to $0.45d_o$ reported for medium sand (Williams et al. 2004). They concluded:that their experiments did not rule out large 3-D hummocky ripples in coarse sediment since 125 cm/s, was the highest oscillatory velocity tested and a significant amount of phase space exists up to the plane bed estimate of 200 cm/s, (Clifton, 1976).

This phase-space gap was addressed by Ruessink et al.(2015) who used a large-scale (15m x 70m) wave-flume with medium to coarse sand (D_{50} = 430 µm) to examine the cross-section and planform geometry of wave-formed ripples under high-energy shoaling and plunging random waves. They determined that the ripple planform changes with the wave Reynolds number (a measure of wave forcing) from quasi <u>two-dimensional vortex ripples</u>, through <u>oval mounds with variably-oriented ripples attached</u>, to <u>strongly subdued 3-D hummocky-type features</u>. Also the ripples remained orbital for the full range of encountered conditions. By combining their data with existing coarse-grain ripple data, they developed new equilibrium predictors for ripple length, height, and steepness suitable for a wide range of wave conditions and a D_{50} larger than about 0.3 mm. Their proportionality between (L) and (*d)* is not constant, but ranges from about 0.55 for $d/D_{50} \approx 1400$ (mild waves) to about 0.27 for $d/D_{50} \approx 11{,}500$ (strong wave forcing).

<u>Paleohydraulic Reconstructions</u>

The collection of wave ripple data (e.g., wavelength, height, grain size, and crest azimuth, if present) can be useful to estimate the general wave climate, shoreline orientation, relative distance to shore, and the number and intensity of storms over a time interval. For example, Banjeree (1996) used HCS wavelength data to assess changes in wave regime and cyclicity at outcrop scale, Ito et al. (2001) used it as a climate proxy over swaths of geologic time, Yang et al. (2006) used changes in HCS wavelengths to demonstrate changes in water depth and distance from shore on a modern open-coast tidal flat, and Keen et al. (2012) used modern hurricane deposition/preservation ratios to estimate storm frequency in Cretaceous HCS strata.

And the general wave climate can be estimated; if the wavelengths of symmetric wave ripples exceeds about 75 cm, then an unrestricted water body such as an open sea can be inferred (Cummings et al., 2009).
More specifically, if limits can be placed on some hydraulic and/or sediment parameters, more precise estimates of paleo-conditions can result. In the present case with a wide range of particle sizes, possible bounds include:

- wave period (T ≈ 8 - 15 seconds) - inferring ancient hurricanes, based on paleo-latitude and given modern data and the moderate fetch of hurricanes, gives an upper bound of T ≈ 15 seconds);
- water depth (maximum ~ 10 meters) - since significant offshore transport of very coarse sediment is estimated to be limited and the shelf gradient is inferred to be low;
- wave height (from wave charts and orbital diameter estimates);
- orbital diameter (d = L/0.4); L = ripple wavelengths, field measured. For sinusoidal waves, d ≈ .wave height
- orbital velocity (derived from d ≈ L/.4 then U ≈ d (3.14)/T) - can estimate particle entrainment limits and transport potential (Fig.), and sediment transport rate (≈ cube of U), and bed shear stress (≈ square of U x drag forces).

Since hummocky bedforms are large 3-D wave ripples, ripple wavelength (L) relates directly to the near-bed orbital diameter (d) and thence to other properties such as the orbital velocity. The L/d relationship is affected by grain size and the ripples must be orbital (i.e., L scales with d; some smaller fine-grained ripples are anorbital). For coarse to medium sands, orbital diameter predictors (L/d=) include Ruessink et al. (0.27 to 0.55), Cummings et al. (0.4), Williams et al. (0.45), and Gilbert (0.5); a rough average gives **0.4 = L/d**.
Rearranging, d = L/0.4 and using HCS wavelengths (L) averaging about 1 m and ranging up to ~ 2 m for most of the sequence gives an orbital diameter (d) = 2.5 m and 5 m, respectively. Orbital velocity, $U_o = \pi d/T$; where $\pi = 3.14$ and T = 10 s (a common wave period for hurricanes) then U_o = 0.8 m/s to 1.6 m/s. These energetic wave excursions are capable of entraining pebbles of about 0.7 mm to 30 mm, respectively (Fig 10; per Komar's chart), 1974. Similar but somewhat higher values were obtained from a similar Mississippian "flat pebble" conglomerate situated about 100 m above the Salamanca conglomerate in the highlands of Allegany State Park (see); all are indicative of large waves/powerful storms.
Significantly larger hummocks (L ≈ 5 to 10+ m) are located in upper portions of outcrops #4 and #5. Maximum pebble size appears to trend with hummock size. The largest and coarsest (some with pebble-bedding and one clast-supported bed w/chaotic fabric in the domal area) are located immediately subjacent to the caprock at outcrop #5 which displays the largest clasts (up to 60+ mm) observed in this study (Fig. 7, 8).

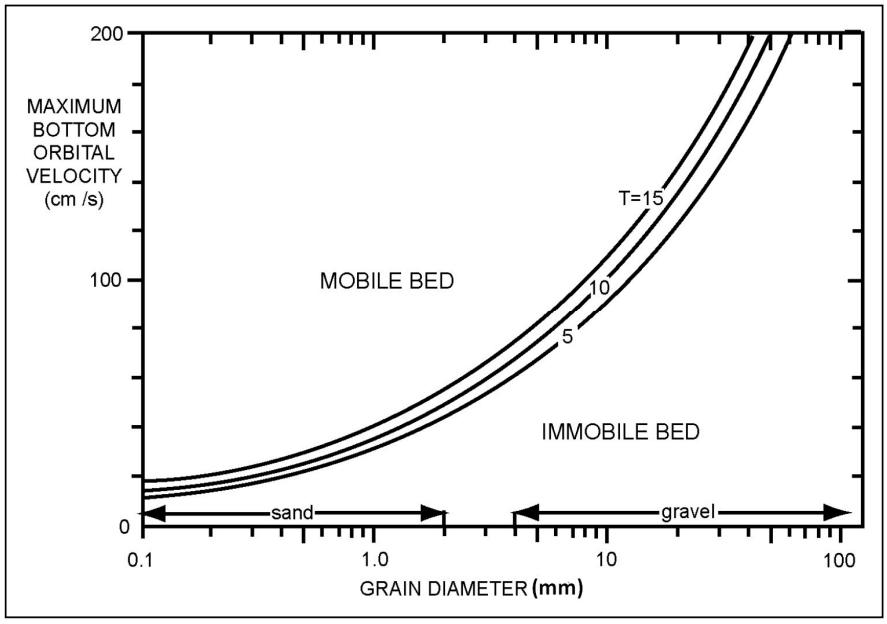

Figure 11. Wave entrainment and bedform stability diagrams

Threshold velocities for sand and gravel under oscillatory flow produced by waves with periods of 5, 10, and 15 seconds. Adapted from Komar and Miller (1973).

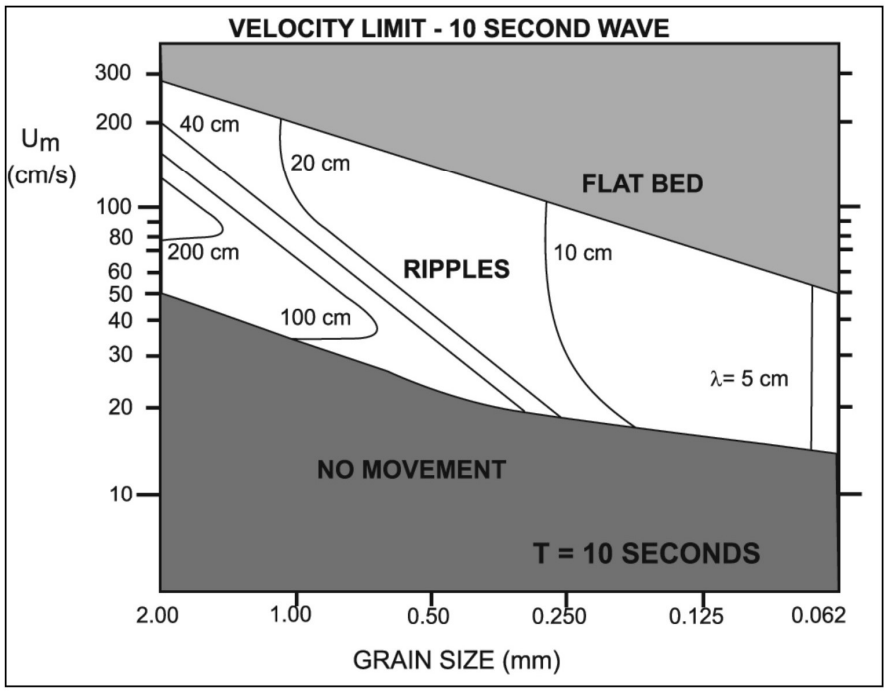

Influence of grain size on bedform under symmetrical oscillatory currents generated by a 10 second wave. Adapted from Clifton (1976).

To assess variability in time and space and look for anomalies, measurements of 53 hummocks from across the outcrop belt were plotted on Fig. below along with orbital velocity values calculated with T= 10 and T = 15 and limits for maximum velocity and plane bed transition.

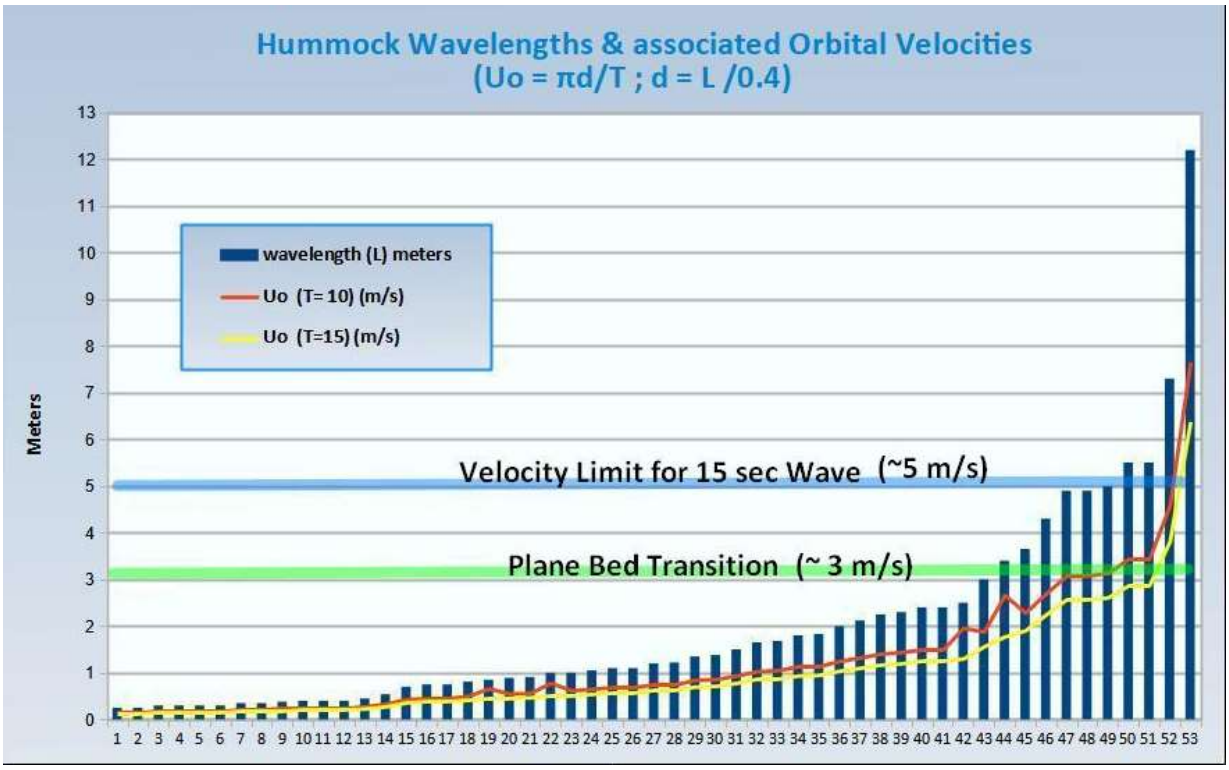

Figure 12. Measured hummock wavelengths with calculated orbital velocities

Velocity estimates for the seven largest hummocks are at or above the expected transition to sheetflow/plane beds (about U_o = 3 m/s for 2 mm sand). Since plane beds were not observed and since pebbly sediment would likely push this transition line higher (especially for more difficult to entrain "flat" pebbles), plane beds are unlikely from oscilatory currents under these conditions. As Clifton (1976) noted, sheetflow in coarse sand is unexpected except in shallow water under extreme conditions. The two largest hummocks exceed the maximum velocity "fence" (about U_o = 5 m/s and 4 m/s for waves of T = 15 and T = 10 seconds, respectively; Clifton (1976; 2003; Fig.10). Unnoticed amalgamation could be a factor or Airy wave theory may not be strictly applicable. And considering the inferred transport of large volumes of coarse sand and pebbles for most HCS and in particular, the coarsest and largest hummocks, combined flows are necessary. With higher potential velocities and bed shear stresses under waves, sediment may be entrained/mobilized and transport may then be effected primarily by unidirectional currents. Several offshore sediment transport scenarios include longshore and tidal currents directed parallel to shore and rip current cells directed offshore and downwelling from storm setup. The effect of combined flow is multiplicative rather than simply additive (Bridge & Demicco, 2008). Mike Leeder (2009; p. 421) summed it up nicely: "Storms generate rip and gradient currents that transport sediment offshore, giving rise to sharp-based, sheet-like, poorly sorted gravels and sands exhibiting hummocky cross-stratification."

Based on the paleo-hydraulic analysis of hummock formation above, plane bed/sheetflow is unlikely under oscillatory flow but antidunes are possible under unidirectional flow. Moreover,

the uniform planar bedding, subparallel with erosional set boundaries cross cutting sets at different inclinations caused by deposition under frequent changes in elevations and slope from waves and tides.
A thickness of 1 to 3 meters suggests a uniform steady process and its stratigraphic position indicates a foreshore/beach origin. Landward of the breaker zone, waves run-up the beach, the swash zone and the return flow is called backwash. Low-angle stratification dipping seaward a few degrees, is produced and generally increasing with grain size. Maximum longshore currents occur in the breaker and surf zones (meters/second). During storms, large volumes of sediment are suspended and entrained by wave/surf action. Longshore currents may readily transport it and with offshore-directed rip currents deliver coarse sediment offshore.

Note: Perillo et al. (2014) provided a predictor of L/d = 0.82 for combined flows for 0.25 mm grain size and Dumas et al. (2005) provided 0.5 for combined flows in fine sands. Since the ripples in their studies remained orbital and the unidirectional component was << than the oscillatory component, the more common oscillatory predictors, with a greater range of grain sizes (the key variable), are preferable.

Equilibrium Times

A surprising result of the unified model of bedform development and equilibrium (Perillo et al., 2014) is that large bedforms reach equlibrium much faster than smaller bedforms apparently due to higher sediment transport flux (and higher associated current velocities). As their flume study showed, large bedforms, such as hummocks required much less time (only a few tens of minutes) to reach equilibrium conditions than small wave ripples which generally required several hours. And they presented four stages of bedform genesis and growth; the second stage ("growing bedforms") showed exponential growth by sediment capture and amalgamation. Large hummocks then may develop quite rapidly and the time represented by individual HCS beds may be measured in hours or less.

The unified model of bedform development and equilibrium under oscillatory, unidirectional, and combined flows (Perillo et al., 2014) that showed bedform equilibium times for all flow types were inversely proportional to the sediment transport flux. Since the flow conditions required for large wave ripples mobilizes significantly more sediment than small ripples, large ripples reached equilibrium faster. This result illustrates that the sediment transport dynamics play a key role in controlling the equilibrium time of bedforms. The experimental results show that the processes of bedform genesis and growth are common to all types of flows independent of bedform size, bedform shape, bedform planform geometry, flow velocities, and sediment grain size. Four stages of bedform genesis and growth: (i) incipient bedforms (e.g., rolling grain ripples); (ii) growing bedforms (e.g., hummocks; exponential growth by sediment capture and amalgamation); (iii) stabilizing bedforms; and (iv) fully developed bedforms (dynamic equlibrium; wavelength and height fluctuate bedforms may merge, split, and produce a relatively large range of active sizes). Based on these experimental results, it was observed that the genesis and growth processes are common for all types of flow.
This model may help explain the presence and growth of small-scale HCS at bases of some larger hummocks (such as outcrop #2 and #5; (Fig. 7). The small forms may be considered "incipent bedforms" which then grew exponentially into large hummocks as flow conditions

allowed, stabilized and in dynamic equilibrium, may form an array of sizes. Arnott & Southard (1990) noted a similar effect where large 3D wave ripples, which grew in size to 1-3 m at the highest attainable U_m of 1 m/s, shifted in position and changed in size with time, seemingly at random, causing substantial local and temporary erosion and deposition at a given point on the bed.

Effects of Pebble Shape

By some measures, such as a simple fluid/particle force balance and frictional considerations, low-profile discoidal pebbles should be more difficult to mobilize Experiments by Komar and Li (1986) showed that pivoting angles are key variables and listed spheres as most readily entrained followed by smooth ellipsoids; angular clasts were last. With smooth discoidal clasts, "rolling" like a sphere is impeded but the typical biconvex oblate ellipsoid shape may be more readily "lifted" and entrained in a current. Once entrained ("mobilized") in a current, the discs would likely settle slower as indicated by calculation of the Maximum Projection Sphericity (Sneed and Folk, 1958). Also known as Maximum Settling Sphericity, a range of pebble sizes yielded about 0.5 (equivalent to about twice the cross-sectional area of a sphere of equivalent volume) which suggests slower settling of discoidal pebbles.

Theory and experiments on the effects of grain shape on settling rates confirm such reductions in settling velocities for discoidal vs. spherical pebbles. For example, Komar and Riemers (1978), Dietrich (1982) and Wu and Wang (2006) showed about a 50 - 60% reduction in settling velocities for one-centimeter discoidal pebbles (~ 30 cm/sec) vs. spherical pebbles (~ 60 cm/sec to 70 cm/sec for) due to larger form/shape drag for discs. Somewhat smaller reductions were noted for smaller particles (e.g, ~ 40% for very fine sand; 0.51 cm/sec vs. 0.82 cm/sec). Overall, reductions in settling velocities would be expected to increase pebble suspension and transport with the potential for shape sorting and association with smaller but hydrodynamically similar particles. With observations of large isotropic HCS with pebble-bedding (Fig. 7; end of spectrum) and high U_o predicted for large hummocks (Fig.12), the suspended load of sediment may include pebbles (as well as saltation). With flow deceleration, settling from suspension may be a major part of the formative process as with fine-grained HCS. And once deposited, the low-profile "flat" pebbles, being more difficult to entrain, may "armor" the hummock and with highly variable storm currents, larger pebbles may then be deposited (localized inverse sorting).

So pebble shape and mass (about ¼ the mass of a spherical clast of the same diameter) may be a primary determinant of pebbly HCS and perhaps help explain its apparent rarity in the geologic record. Given that typical shallow-marine strata with typical fine-grained HCS sandwiches the Salamanca, a rapid change in wave climate is unlikely to account for conglomeratic HCS is unlikely. Rather, under intense storm waves, fine sand may stay suspended or develop sheetflow until conditions allow deposition as HCS. With the availability of coarse sand and discoidal pebbles (which would not likely develop sheetflow but orbital velocity limits may be approached as noted above) may allow formation of HCS in the phase space of near sheetflow conditions under full-storm conditions. Sediment shape, size, and mass may help explain large-scale coarse HCS, the largest of which is at the top of formation where inferred shallower water depths may also have been a factor.

Whereas the hummocks appear fairly symmetrical, the evidence of unidirectional currents is abundant (angle of repose cross-beds, high sediment transport and depositional volumes, large

clast transport (ideally one would expect some asymmetry but outcrop orientations are variable).
In any case, given the overall range of coarse hummocky forms, significant sediment transport is evident in these HCS layers (which varies with the cube of velocity) along with deposition (by combined flows decelerating spatially and temporally) in definitive patterns (variably-sized hummocks with similar bedform indices) in a relatively brief periods of time (probably hours to days). And, this exercise highlighted some unusual forms that suggest unusual depositional conditions in this area just below the caprock (a probable "maximum regressive surface" or "transgressive surface" depending on one's view).

Giant Ripples of the Medina

Gilbert (1899) was apparently the first to describe the type of cross-bedding now known as hummocky cross-stratification (HCS) and moreover, the first to deduce and reconstruct possible wave conditions for ancient deposits. As he observed in Medina sandstone quarries and outcrops near Lockport, NY, the cross-bedding is "*a peculiarly intricate type, exhibiting dips toward all points of the compass in the same quarry, and associated with it are many unconformities*" (random cross-bedding/truncations which made these beds unsuitable for building stone). In a quarry, the strike and dip of a layer *"can be traced through an elliptic arc, like the end of a spoon for 150 degrees"*. *"In width* (wavelength), *these giant ripples range from 10 to 30 feet; in height, from 6 inches to 3 feet. Their material is a sand of medium grain."*

FIGURE 1.—GIANT SAND-RIPPLE
Occurring in upper sandstone lens of the Medina formation at Lockport, New York, exposed in old quarry west of the Indurated Fiber Works

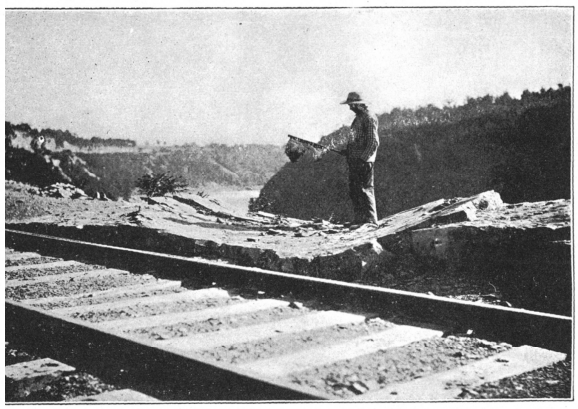

FIGURE 2.—GIANT SAND-RIPPLE
curring in "quartzose sandrock" of the Medina formation, exposed in the Niagara gorge, one mile above its mouth. New York Central railroad track in the foreground

GIANT SAND-RIPPLES

(Historical fotonote: The 1888 invention of roll film and affordable/portable cameras in Gilbert's hometown must have transformed fieldwork just a few decades after the classic 1843 Geologic Survey of New York relied on exquisite but tedious hand-drawn illustrations. A century later, Kodak invented digital photography, again transforming the landscape and driving innovation (and personally, filling hard drives, bereft of Kodachrome). And this centennial tribute to Gilbert's myriad geologic contributions is illuminating: https://eos.org/features/reflections-on-the-legacy-of-grove-karl-gilbert-1843-1918).

Bedding plane exposures of the giant ripple bedforms were/are uncommon as with most bedrock outcrops. But building stone quarries were common before the advent of concrete and the quarry floors presented early geologists with the rare plan view/third dimension as might be otherwise seen only in shallow rock-floored streambeds. The example depicted in the left photo above includes two crests and an intervening trough; the trough is 23 feet across and 29 inches deep. A partial exposure shown in the right photo shows a trough fragment 15 feet across and 16 inches in depth. And another quarry exposure reportedly showed a bedform with a convex crest 15 feet across. The associated cross-bedding (n.k.a., HCS) however, is common in vertical outcrop exposures of Medina sandstone between Lockport and the Niagara gorge and elsewhere (from which measurements of "apparent" wavelength can also be attained).

In a series of deductions based on nascent wave-ripple experiments (e.g., Darwin, 1883/84; son of Charles; "ink mushrooms/trees" discussed at length in Allen, 1982) of the day and his own observations, Gilbert surmised that these bedforms and cross-bedding formed by *"sand rippling, differing in no respect except size from the familiar ripple-mark of the bathing beach…the cross-bedding is a result of deposition during the maintenance of a rippled surface on the ocean bed, and the unconformities record the readjustment of the sand ripple pattern when the controlling water movement assumed a new direction."* He further noted that the orbital motion induced by waves becomes elliptical near bed and *"the frequency of the natural oscillation equals the frequency of the wind waves, and its amplitude is a function of the size of the waves and the depth of the water...so that a relation will ultimately be established between wave-size, wave-period, and water depth as conditions and ripple-size as a result."* He presciently summed up the crux of the wave/ripple-mark conundrum. Gilbert concluded that at the most, ripple-mark wavelengths are about half of the wave height. And he humbly noted that if this relationship is substantiated by future research, "*the geologist may infer from the structure of the Medina sandstones that the Medina ocean was agitated by storm waves sixty feet high. As great waves require broad and deep bodies of water for their generation, such a result would demonstrate the association of the Medina formation with a large ocean.*"

Some six score years later and a tsunami of wave research, unique solutions for ripple size from wave size, period, and water depth are still lacking but useful estimates can be had with paleo-depth inferences and wave and sediment constraints. Most modern predictors of ripple wavelength (L) vs. wave orbital diameter (d) ≈ sinusoidal wave height) use a relation which ranges from about **L/d ≈ 0.3** to **0.8**. Gilbert's prescient predictor of **L/d ≈ 0.5** appears "substantiated" and we may infer that the sedimentary structures he recorded (ripple wavelengths of 10 to 30 feet) were formed by storm waves on the order of 20 to 60 feet high in an unrestricted ocean of some depth. Such wave heights are common in large storms according to hurricane data collected over the last few decades (an eye blink, geologically). For example, significant (highest 1/3) wave heights range roughly from 10 to 20 meters for Category 3 to 5 hurricanes. Ocean buoy data collected during Hurricane Katrina showed significant wave heights of ~ 17 m (55 feet); statistically, the highest waves could have been as high as ~ 32 m (105 feet). Similarly, wave periods are elevated for large hurricanes averaging at least T = 10 seconds within a 100 km radius of the eye and T ≈ 15 seconds near the eye (https://sos.noaa.gov/catalog/datasets/wave-heights-hurricane-katrina-2005/).

Description of Unidirectional Current Structures - Subaqueous Dunes and Bedload Sheets

Unidirectional currents (e.g., streams, tides, longshore/rip cuurents) are ubiquitous in nearshore environments. With bedform formation and migration, cross-stratification of various styles and sizes result. Dunes scale with flow depth (pint to building size here) and bedload sheets are low profile (few grains high) bedforms which transport mainly pebbles. Other common bedforms such as ripples and upper-stage plane beds occur in finer-grained sediment (~ < 0.6 mm) that is uncommon here. Likewise, upper-flow stage antidunes are possible (with high velocities and shallow depths) but with pebbles, transverse ribs would be expected and were not observed.

Large-scale Cross-stratification

Cross-stratification is present in most and dominates some outcrops. Individual set dimensions range over two orders of magnitude in scale (~ 0.10 m to +5 m). Most cross-strata are planar (i.e., straight- to slightly- crested = 2D type) with some trough (i.e., sinuously crested = 3D type = higher flow stage) evident in channel deposits and upper shoreface/lower foreshore deposits.

Foresets are largely composed of grayish medium to coarse sand with variable interbeds of milky granules and pebbles ("grain striping" within large-scale foresets). Larger sets are generally coarser. Some channel bars and fills are composed in large part with pebbles (open framework gravel) that are crudely stratified or imbricated.

The vast majority of paleocurrent data are cross-bed inclinations and range from 90^{o}– 150^{o} (mostly) with minor clusters at 40^{o} – 60^{o} ; 170^{o} – 190^{o} (coast parallel); 220^{o} – 240^{o}.

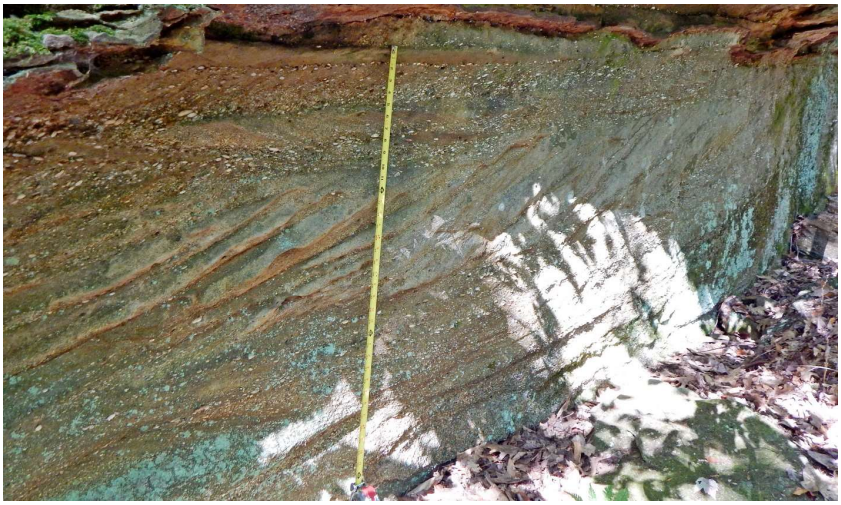

Figure 13. Bi-directional cross-bedding at top; tidal bar ; tape = 1 m – outcrop #7.

The largest cross-strata (0.50 – 5 m) increase in size and abundance from north to south across the outcrop belt. At the southernmost outcrops at "Little Rock City", large foresets may comprise ~ 75% of the outcrop exposures with dips of 20^{o} – 30^{o} and no obvious or major

reactivation surfaces. Most toesets are tangential. Some foresets are traceable for +150 m across several blocks and a planar truncation surface at the top of the dunes shows wave influence (e.g., wave ripples with crests parallel to the paleo-shore and HCS beds above).

Figure 14 . Largest dune (+ 5 m) observed at LRC - outcrop # 7.

Interpretation of Cross-Strata

Hall's (1843) explanation of "diagonal lamination": *"...where the sand is carried on and spread over the surface, sloping off towards one side farthest from its origin. The next deposition covers this sloping side necessarily in the same manner, producing the oblique lines..."* was the first documented account of cross-stratification (Allen, 1982); it describes the essential process of sand movement and deposition on an inclined surface. To embellish slightly, currents transport sediment along a gentle stoss slope to the bedform crest where repeated sediment avalanches down the steeper lee slope form cross-strata at or near the angle of repose. The resulting cross-strata are the depositional units formed by the migration of bedforms, dunes of various scales in this case.

Based on mostly shoreward- and some bi-directional-oriented cross-strata, the dominant currents were tidal and predominantly flood tides. Most sediment transport likely occurred during high spring tides of the bi-monthly spring-neap tidal cycle. Bedload transport rates scale roughly with the cube of the current velocity; if the flow rate doubles, bedload transport increases by a factor of roughly eight (Wang, 2012). A mesotidal range of 4 m appears to be a reasonable estimate; similar modern deposits/bedforms are produced in that range such as in the North Sea.

Paleohydraulic Estimates for Unidirectional Currents

As discussed above, discoidal pebbles are likely more difficult to entrain but also settle about 50% slower. And their mass is about 60% -75% less than a sphere of the same diameter. Overall, reductions in settling velocities would be expected to increase pebble suspension and transport with the potential for shape sorting and association with smaller but hydrodynamically similar particles.

Bradley et al. (1972) studied the effect of shape both in the field (Knik River, Alaska; high-gradient glacial-meltwater stream) and in the laboratory. They detected downstream sorting of shapes, with platy pebbles being the most easily transported, then elongate pebbles (rollers), and more equant pebbles being the least easily transported. The different shape-sorting effects were attributed to particles moving by traction and by suspension and hence closely related to flow strength and particle size.

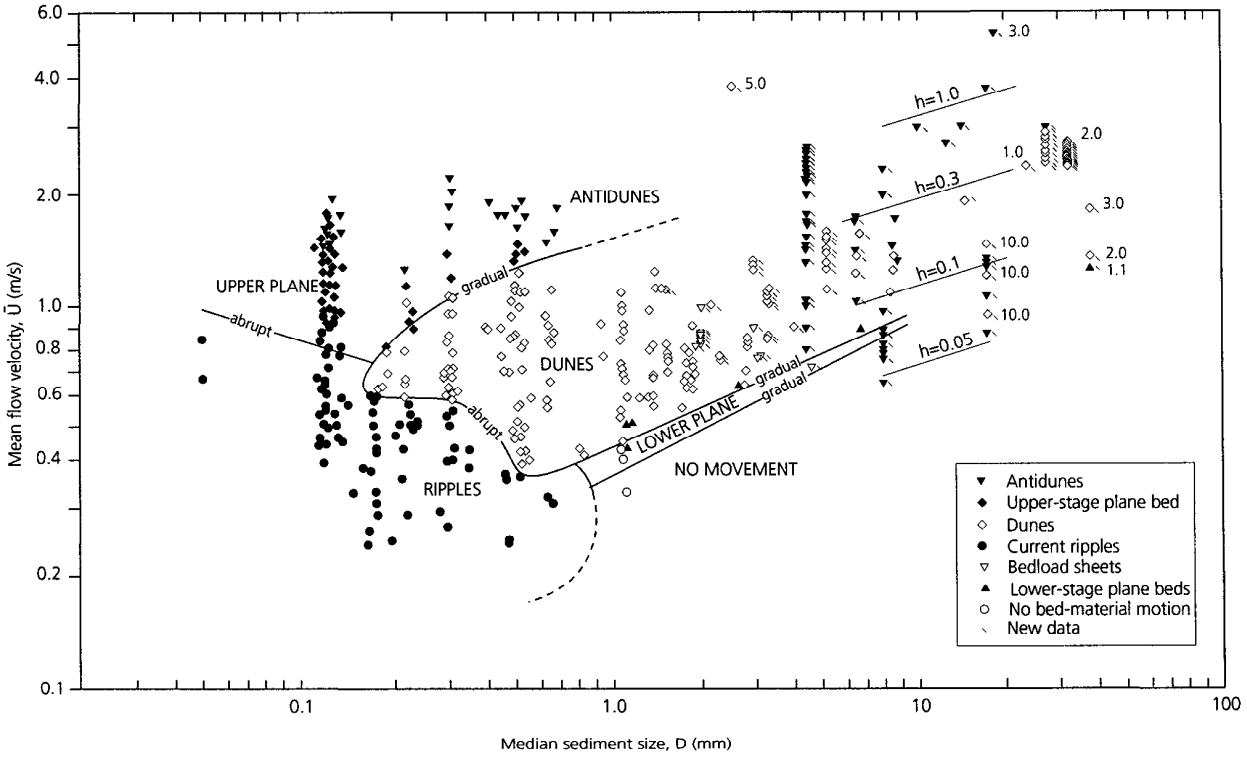

Figure 15 - Bedform Existence Fields for Unidirectional Flows (Carling, 1999; redrawn after Southard and Boguchwal, 1990 and extended to gravel sizes, D ~ 33 mm). For general background, see Middleton (1977), Allen (1982), and/or Harms et al. (1982).

The bedforms most applicable to conditions at LRC are Dunes and Bedload Sheets. Dunes of various dimensions produce cross-strata which incline downcurrent and scale with depth, flow strength, and grain size. Ripples, smaller-scale (<= 4 cm) dune-like bedforms, require sand of < ~0.6 mm which is uncommon at LRC; ripples have not been observed. For sand sizes, a current of roughly 0.4 m/s to 1.0 m/s would be required to form dunes. For dunes composed of granules and fine pebbles (2 mm to 8 mm), a current of 0.6 to 1.5 m/s is indicated. Flows required for coarser pebbles (8 to 32 mm; limit of graph) are less clear given prominent disc shapes and data scarcity, but currents of 1 m/s to +2 m/s appear likely. Bedload sheets, low-amplitude bedforms which can transport a range of sediment are likely common at LRC but difficult to definitively identify; their existence field appears to coincide with dunes.

Based on paleohydaulic estimates noted above, the currents required to form dunes ranged from about 0.5 to 1.5 m/s. A similar velocity range (0.5 - 1.0 m/s) has been reported in the Dutch North Sea where very large simple dunes (like those at LRC) are actively migrating

decimeters to a few meters per year (e.g., Tonnon et al., 2007; Passchier and Kleinhans, 2005; Stride, 1982). Allen (1982) reported that on the European continental shelf, sandwaves (large dunes) are found where tidal currents associated with spring tides range between 0.65 and 1.30 m/s. LRC dunes are somewhat coarser than modern examples and perhaps formed in somewhat shallower depths. A shoreface depth of ~ 10 m would conform with the dune height/depth ratio of 0.5 (Allen, 1982) for the largest (~ 5m) LRC dune (note that lower *h/d* ratios are the norm; Reynaud and Dalrymple suggest ~ 0.2). But it is unclear how smaller superimposed dunes (sediment "caravans" that migrate up the stoss slope of the large dunes delivering sediment to the avalanche face) affect this estimate; these would scale to a much shallower depth.

Tidal transport of coarse sand and pebbles at much greater depths may have been limited by the "littoral energy fence" whereby coarse particles are sequestered nearshore (Allen, 1970; Thorne and Swift, 1989). Even sand is rarely transported offshore by fair weather processes but evidence for Devonian hurricanes in the Catskill basin is strong and modern studies of sediment transport inform the past (e.g., Keen et al., 2012).

Figure 16. Large dunes at Little Rock City, outcrop #7. This series of blocks form one dune > 125 m long with foresets ~ 4 m high. Considering the very consistent flow direction and steady sediment transport rate (reflected in fairly uniform foresets) and formation over decades to centuries implicate tidal currents.

The large foresets on large "simple" dunes suggest strong very asymmetric tides. Allen (1980, 1982) depicted four general variants of "sandwaves" (what geologists now call "dunes" per Ashley, 1990) based on tidal current symmetry. Allen's conceptual "sandwave"/dune generated by the most asymmetric tides (Fig. 16; large simple foresets in bottom frame; note the velocity asymmetry of U* critical, the threshold velocity to move sediment) conforms with the large dunes at LRC. Allen (1982) also depicted superimposed smaller dunes supplying sediment to the large foresets of a larger host dune.

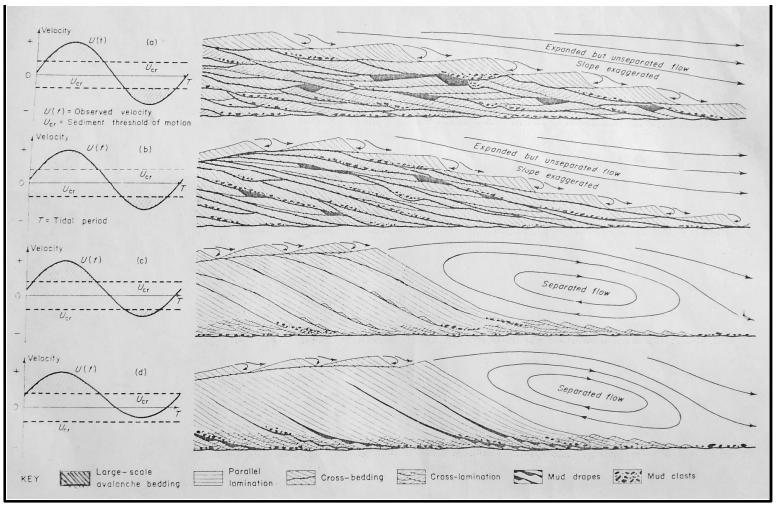

Figure 17. Conceptual Model for generation of large dunes (Allen, 1982)

The formset dune at the LRC dune field contains a small dune that appears to have "stalled" at the crest and reformed/"sharpened" it (center of Fig. ; above 18 cm ruler); deposition continued along the aligned stoss and lee of both dunes (cf. Bridge and Demicco, 2008). Superimposed dunes pre-sort and transport sediment to and over large host dunes often in concert with bedload sheets. Pre-sorted wedges of sediment, as formed by smaller dunes ("trains") advancing over the crest ("cliff") of large host dunes, move down the flow-separated lee slopes often haltingly, by "grainflow" and finer sediment is distributed by "grainfall" from suspension (Reesink and Bridge, 2007; 2009).

One consequence is the scattered formation of lobate tongues of coarse sediment that may show sorting and inverse grading due to kinetic sieving. Otherwise known as "grain striping" (Reynaud and Dalrymple, 2012), a likely result of this process is shown in the dune cross-section along depositional strike (dune "backside") with scattered and variable convex piles of granules and pebbles along the foresets.

Harms et al. (1982) described the process of foreset avalanches at high sediment concentrations as oversteepened areas which slump in places and slide down the lee slope as long "tongues". A slight scour or channelized grainflow may form which then "debouches" with a slight positive lobe at the basal portion of the foreset. Some foresets and "grain stripes" at LRC nicely display these subtle structures in dip cross-section (Fig.10) and the small granule "piles" on a dune backside noted above are interpreted as "grainflows" along the strike of dune foresets (Fig.18, below).

Figure 18. Above: Humps of coarse sediment (grainflows from subordinate dunes) along depositional strike of the dune. Some humps show inverse grading likely from kinetic sieving during foreset avalanching. Right, large dune displays “grain striping” produced by grainflow of coarser sediment (tan granules in this case) down the foresets.

The largest cross-strata (0.50 – 5 m) increase in size and abundance from north to south across the outcrop belt which may indicate increasing water depth since dunes scale with flow depth. And the LRC dune field is downcurrent (longshore, tidal, and possibly storm setup) of the inferred delta complex which provided an abundant sediment supply and may partially explain the location of the dune field.

Figure 19. Form-set Dune

The form-set dune at the LRC dune field contains a small dune that appears to have "stalled" at the crest and reformed/"sharpened" above 18 cm ruler; deposition continued along the aligned stoss and lee of both dunes (cf. Bridge and Demicco, 2008).

Superimposed dunes pre-sort and transport sediment to and over large host dunes often in concert with bedload sheets. Pre-sorted wedges of sediment, as formed by smaller dunes ("trains") advancing over the crest ("cliff") of large host dunes, move down the flow-separated lee slopes often haltingly, by "grainflow" and finer sediment is distributed by "grainfall" from suspension (Reesink and Bridge, 2007; 2009).

In this case, it appears that a medium ebb-dune formed at the base and small competing dunes aggraded vertically (or slightly in the ebb direction) until the flood (shoreward) tides began to dominate about where the small dune is perched in the middle of the bed. With an abundant up-current sediment supply, the flood tidal current began to dominate and the ~ 2–3 m dune began to migrate. In effect, the simple large dune has compound small dunes at its core/start and other superimposed dunes supplying and presorting sediment probably along with bedload sheets. In addition to a small dune in the topset bed, at least 2 topset locations show continuous strata between inferred bedload sheets and foreset beds. In a review of dune preservation, Reesink et al., (2015) noted that dune sets may climb due to local dominance of deposition over dune migration which generally fits this situation. But more specifically in this case, it appears that the localized balance between ebb and flood dune deposition aggraded a vertical core until the more dominant flood current and sediment supply tipped the balance toward large dune migration.

Wave-truncated Dunes

All of the largest dune (> 3 m) foresets at LRC appear to have been truncated ("beheaded" dunes) horizontally at similar elevations (~ 3 – 4 m from the top of the sequence). Evidence of HCS (see below) and wave ripples at this interface is common which suggests storm wave

action, as well-documented in the North Sea (e.g.,Terwindt,1971; Reynaud and Dalrymple, 2012).

Figure 20. About one meter of uppermost dune is exposed and appears truncated, followed by 0.75 m of HCS and (on the left) about 1 m of low-angle strata which is truncated and followed by HCS red beds and capped by a 0.5 m pebble-rich stratum (caprock). Two storm wave truncation events are interpreted.

Channel Deposits

Figure 21. Large channel complex at outcrop #6. Marine strata w/HCS at base, large channel-form above. Multiple channelss, some incision (tape = 1 m); deltaic depositional environment inferred.

Channel deposits comprise upper portions (uppermost ~ 1 - 3 m and up to ~ 5 m at outcrops #2, 3 & 6) Low-angle stratasets and associated channel-forms/fills dominate these deposits.

Low-angle stratasets (a.k.a. "lateral accretion deposits"; LADs):

- dips ≈ 10 -20^{o} (up to 25^{o});
- are typically 2- 4 m thick, measured normal to bedding;
- extend laterally tens or up to hundreds of meters; and
- may be organized/stacked vertically into several "storey" units.

Individual strata/beds of low-angle stratasets:

- are centimeters (cm) to decimeters (dm) thick;
- vary in cross-sectional shape from co-planar (mostly) to gently concave-upward (as beds may thicken along dip) and rarely convex-upward; and
- display planar (normally-graded) stratification and cross-stratification with some alternating bi-directional foresets in places) and cryptic or massive bedding where pebbles dominate.

Figure 22. Three low-angle stratasets (identifible by color and bedding style) stacked laterally over /
horizo.ows two small wave ripples at top; the center set dips ~0° (local flow ≈ E-W and contains pebbly cross-strata directed southward; on the left, gray thinner-bedded set incised the center set and dips ~45° (local flow ≈ NW-SE) and the bedding shows arched weathering (possible wave influence); and chilling human standing on mounded HCS caprock.

Figure 23. . Outcrop #3 – Apparent preservation of a curved channel-form and adjacent curved low-angle strataset (an intact point bar/channel deposit).

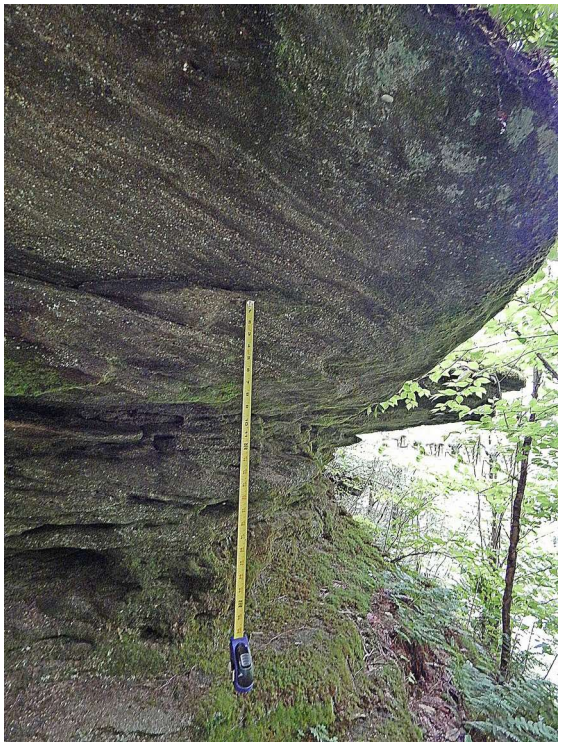

Figure 24. Top – Low-angle strataset (point bar) of large channel complex ; 5 m deep channel inferred, outcrop #3. Above – Head on view of same,. Right – Smooth channel-form, outcrop #2 (tape = 0.7 m).

Channel-forms are very common with basal surfaces which curve gently downward from truncation/pinch points (apparent channel tops/sides) into sub-horizontal planes (channel bottoms). Some incision and scouring (lag deposits) along channel bases are evident especially where channels cross-cut and stack vertically. Rarely, terraced or two-stepped channel sides were observed at outcrop #6. The contacts of basal channel deposits with wave-ripple and hummocky cross-stratified deposits (observed at outcrops #2, 3, and 6) show little relief and are essentially horizontal at outcrop scale. The symmetrical (most common) to asymmetrical wave ripples and hummocks (heights ~ 10-20 cm; wavelengths ~ 20-80 cm) are typically finer-grained (dominantly fine to coarse sand) than overlying channel deposits but pebbles are found throughout.

Interpretation of Channel Deposits:

• The low-angle stratasets are interpreted as "point" bars which migrated by erosion of cut banks and deposition on the point bars (i.e., lateral accretion deposits; LADs). The rate of movement/degree of meandering depends a number of factors such as stream gradient, bank stability, flood frequency, sediment bedload and suspended load.

• Channels and point bar deposits are well exposed in places. The sense of flow direction is less clear but bi-directional cross-beds are present. At outcrop #2 and #6, some channels weather out and overhang dramatically with steep (> 45^{o}) sides; some joint surface exposures are much less obvious.

• The general E-W strike of strataset beds indicates overall E-W orientation of meandering channels. An exception is several (likely-related) outcrops near the NW corner of outcrop #3 which dip generally eastward indicating a general N-S flow direction.

• One such outcrop, a large strataset of 5 m vertical thickness which overlies the mouth bar (Fig. 25), showed a sequential 90^{o} variation in stratal dips (120, 90, 60, 30^{o} upward) This swing equates to NE-SW, N-S, NW-SE, NW-SE change in flow directions for a meandering stream reach over time. Four LADs are apparent and distinctive and may represent stream and delta plain incremented response to relative sea level change. Alternatively, the relatively small direction change may indicate low sinuosity for a relatively large ($\sim$ 5 m deep) channel (probable distributary) which likely fed the mouth bar deposits beneath it. The individual strata are very coarse but display little structure, mostly flat pebbly beds of possible bedload sheet origin.

• Cross-strata dipping largely E-SE indicates a dominant current flow and associated dune migration toward the SE (shoreward) within channels.

• Bi-directional and shoreward-oriented cross-strata within channel bars/deposits is indicative of tidal currents with a dominant flood component.

• Stratification variably composed of ubiquitous pebbles (2-20mm) suggests transport by strong tidal currents with a significant tidal setup (probably meso-tidal range [2m-4m] or more as corroborated by thick foreshore deposits and very large-scale dunes elsewhere).

• Abundant low-angle stratasets and intermingled channel-forms suggest significant lateral channel migration and frequent channel avulsions as might be expected with non-cohesive channel banks and strong flood tides (directionally-opposed to ebb/fluvial currents in sediment-choked channels).

• The apparent dominance of flood-tide currents in channel and other deposits (e.g., tidal flats/delta plain and large dunes) suggests these outcrops expose a roughly shore-parallel swath through a deltaic complex

• The coarse-grained wave-ripple laminated and hummocky cross-stratified deposits observed in at the base of some outcrops formed by wave/combined-flow currents under open marine conditions as suggested by larger-scale bedforms and inferred formative waves with large orbital diameters and periods.

• The facies relationships and relatively smooth/low relief contacts between the basal channel deposits and the wave-formed marine deposits suggest a low gradient/gradual progradation of a complex of channels and associated deposits onto a low gradient marine shelf.

• Thick lateral accretion deposits exposed over a 200 m stretch of outcrop #3 and ending in a massive channel complex ($\sim$ 5 m deep) are suggestive of a large distributary oriented roughly W-NW.

• Bridge (2000) noted that Devonian Catskill river channels were smaller near the coast (i.e., sinuous, single-channel rivers, tens of meters wide, maximum depths of 4 - 5 m, sinuosity of 1.1-1.3, mean bank-full flow velocity of 0.4 - 0.7 m/s) and perhaps distributive (delta-related). With increasing distance from the coast, slopes increased, rivers became wider (up to hundreds of meters), deeper (up to 15 m), coarser grained, and possibly braided. In this study, two large channels were identified along outcrop #3, one associated with a mouth bar complex and the other about 600 m south on the Rim Trail. Based on point bar deposits, a depth of about 5 meters was inferred for both channels. Given their proximity and progradation over marine deposits, these paleo-streams are interpreted as distributaries.

• The paleo-sea level established by the beach deposits at outcrop #2 correlates with that for the interpreted mouth bar at outcrop #3 (about 5 m below the vertical control provided by the caprock). Given that sea level must have risen at least 5 m (likely on the order of 10 m) in order to form very large-scale HCS that is present at and just below the caprock with thin-bedded wave cross-laminated sandstones present on top (outcrop #5). An estimate of time for this relative sea level rise could be bracketed by the lateral accretion deposits (LAD) within the point bar above the mouth bar. Assuming that one LAD represents one flood deposit (Bridge and Demicco, 2008) or (count each distinctive stratum) and that hurricanes are the causal agent and recur on the order of 2 years (Fielding et al., 2005; for major flooding) or 10 to 50 years (Keen et al. 2006, 2012; for major storms yielding storm beds), counting the LADs (and/or each sedimentation unit) could provide a time estimate.

• Tidal channels and inter-channel tidal flats are inferred but few examples have been identified. The overlap in properties and often cryptic coarse strata present difficulties but more uniform LADs and a flared channel openings , if visible, might be helpful. Subtidal areas are most likely to be preserved and most tidal-flat deposition results from lateral accretion in

association with progradation of the flat and the point bar associated with meandering tidal channels. Therefore, much of the sedimentary record for tidal-flat successions is comprised of features associated with channel fills and tidal point bars.

Mouth Bars

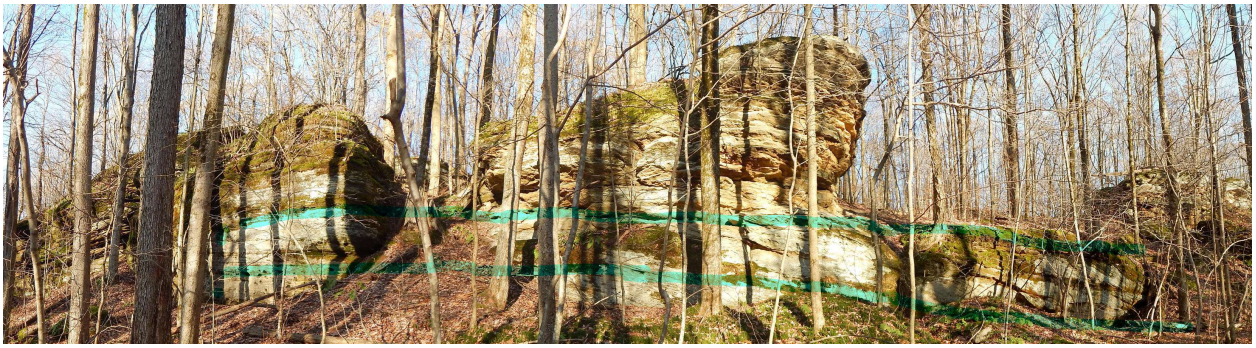

Figure 25. Mouth bar complex forms a bench beneath large channel deposits (outcrop #3 at the south turn on the Rim Trail)

Description

At the base of outcrop #3 where the Rim Trail turns south, three partially-exposed sigmoidal cross-bed sets downlap at low-angles. The overall coset is about 3 meters thick and two major bedding planes which separate sets dip at about 5°. The sigmoidal cross-bed sets average 0.5 - 1 meters thick with low-angle (~ 10-15°) cross-bedding oriented southward. The cross-strata are coarse to very coarse sandstones with thin (~ 4 mm) granule layers usually separating each stratum which average ~ 4 - 6 cm in thickness. Both inverse and normal grading is present with some pebbly strata in places. Set boundaries/major bedding planes are sharp with minor pebble lags and small wave ripples in places on the bases; apparent dip is about 5°. The basal set shows a large (~ 2 m) hummocky form at the updip end and the uppermost set top appears truncated with a large-scale ripple or a small channel. A sinsuous tube-like feature (perhaps a weathering feature) conforms with the top of the basal bed. These sigmoidal cross-beds transition laterally updip (~ 5°) along the major bedding planes into medium to thick-bedded coarse-grained trough cross-beds and HCS which are located directly beneath thick channel (low-angle stratasets dipping eastward) deposits.

Although not directly exposed, thick (2+ m) tapering beds of pebbly, massive and/or partially stratified (e.g., arched pebbles/HCS, Fig.) conglomerate are situated along the outcrop base north and south of this exposure and appear to correlate with it. The base of the conglomerate unit is sharp and irregular and is subdivided in places by bedding planes or thin sandstones; total lateral extent is about 200 meters.

Figure 26. Mouth Bar Deposits: (A) Coset of sigmoidal x-strata; sets are over/downlapping (tape = 1 m). (B) Same as A in a float block. (C) Tapering amalgamated conglomerate beds, 2+ m; fining upward; large (L = 2+ m) isotropic pebble-laminated hummock/HCS suggests storm waves were active during formation/deposition; tape = 1 m. (D) Similar to C but more massive bedding some wavy strata above the erosive base; tape = 1 m.

Interpretation:

The downlapping sets of sigmoidal-cross stratification and associated trough and HCS cross-strata and the massive conglomerate unit, all located subjacent to large fluvial lateral accretion deposits (point bar/stream-reach = N-S orientation) deposits, are interpreted as mouth bar deposits related to sediment-laden floodwaters entering seawater. With stream flow expansion and deceleration, the coarsest sediment is deposited rapidly, i.e., pebbly fluvial bedload (conglomerate). Sequentially, sediment is sorted and deposited via bedload/traction processes (coarse-grained trough cross-beds transition to moderately-sorted sigmoidal cross-beds) with bypass of finer sands, silt, and clay as suspended loads. Both hyperpycnal and hypopycnal (density-constrast) flows may result from sediment-rich floodwaters whereby dense flows provide driving forces for traction and suspended loads and hypopycnal flows carry plumes of suspended sediment basinward. Marine processes, such as waves, tides, longshore, and rip currents, and storm setup with offshore downwelling or a geostrophic flow may then rework and/or redistribute these deltaic sediments as near and offshore marine deposits.

Ancient examples - In an array of process facies models, Tinterri (2011) noted an association of large-scale sigmoidal cross-strata with mouth bars and hyperpycnal flows as generated by sediment-laden floodwaters entering seawater. His sigmoidal cross-strata descriptions and examples are similar to the Salamanca occurrence. And as shown below, he posited a possible genetic connection between sigmoidal (mouth bar) and hummocky (delta-lobe) cross-strata via hyperpycnal and bypass flows and oscillatory pulses of floodwaters. In a polygenetic HCS review, Jelby et al. (2020) proposed a similar process (hyperpycnal flows and pulsations) for the origin of their gravelly “complex” HCS.

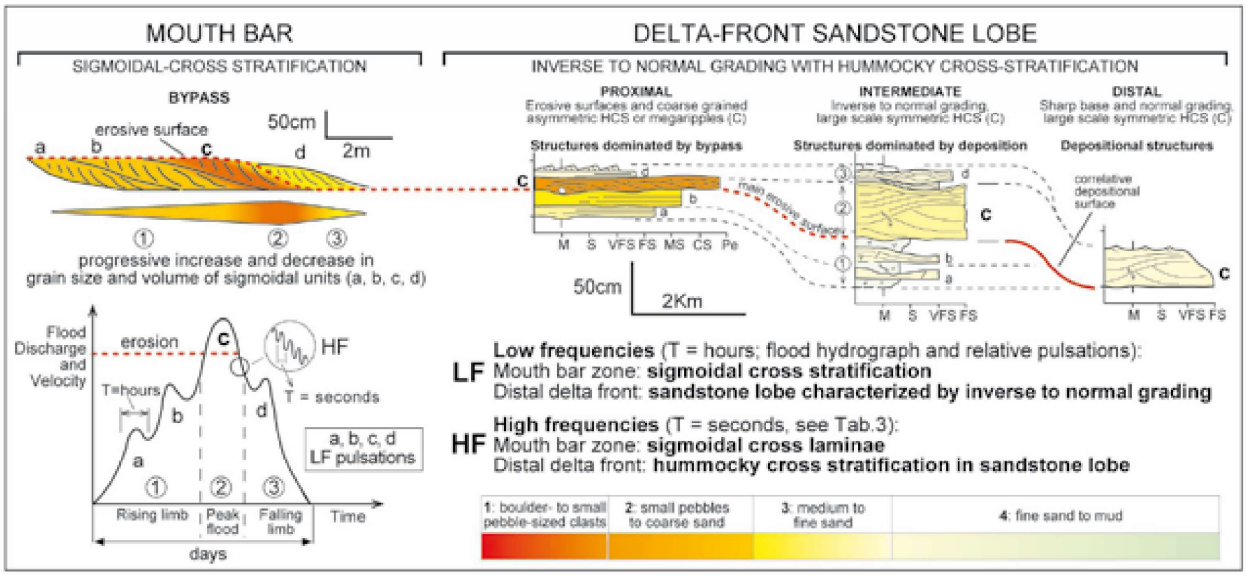

Figure 27. Proposed processes for stratal changes from mouth bar to delta front (Tinterri, 2011)

Modern/recent examples - With separate sets of overlapping/downlapping sigmoidal cross-beds divided by major bedding planes (Fig.) observed at outcrop #3, flooding events are interpreted and the upper bedding plane orientation (~ 5° southward) likely reflects the delta clinoform. Corroborating evidence comes from studies of the Australian Burkedin River and delta which are subjected to episodic flood events, mainly cyclone related (every 1 to 2 years on average) and a wet-dry monsoonal climate. Some floods transport up to several million metric tons of sediment in a few days (Fielding et al., 1999). In a study of the delta, Fielding et al. (2005) surveyed mouth bars with ground penetrating radar (GPR) which showed low-angle dips (1°) on downlapping reflections with steeper dips locally and a major bounding surface, also dipping seaward 1-2°, that separated two distinct inclined bedsets. These results were interpreted as two mouth bars (each ~ 5 m thick), the upper of which overlapped the lower and downlapped along a bounding surface (a low-angle clinoform) in a seaward direction (very similar to the smaller-scale Salamanca examples). They noted that in most places, the mouth bars are sharp-based, typically 4–6 m thick, of moderately sorted sand, and display an equilateral to elongate triangular planform over an area of several square kilometers. Further, mouth bars accumulate on a time scale of 10s of years, with much of the sediment being delivered rapidly during a small number of high-magnitude, short-duration, fluvial discharge events (each of only a few days duration). Supplied by such floods, Burdekin mouth bars aggrade and prograde onto a shallow, low accommodation shelf.

Salamanca delta analogs

The Burdekin River and delta is one of the larger drainage basins on the northeast Australian coast with a drainage area of about 130 km^2 or about 3 times larger than that inferred for the Salamanca study area (and the relative size of the mouth bars roughly scaled)

As noted above, the Arafura Sea and northern Australia is considered a modern analog for the epeiric Catskill sea and coast (Dott and Batten, 1980; Woodrow 1985). Situated on an intra-

cratonic platform, the area is subjected to episodic cyclones (hurricanes; (Fig. 29) and a monsoonal wet-dry climate. In a predictive study of the the Australian coast, Harris et al. (2002) noted that episodic flooding, due largely to cyclones, occurs in generally small, arid, "flashy" drainage basins (50,000 to 130,000 km^2) along the northeast and Gulf of Carpenteria coastlines. Based on estimates of tidal, wave, river power, deltas were characterized as wave and/or tide-dominated. However, they noted that sediment flux rather than river power may exert a primary control on the overall geomorphology of clastic coastal depositional environments, as hypothesized by Dalrymple et al. (1992). The work of Fielding et al. (2005) and others supports this view and hence they classified of the Burkedin delta as "flood-dominated" with wave-influence. Likewise, the Gulf of Carpenteria deltas can be considered flood-dominated, built by rapid sediment flux during large episodic flooding events (major cyclones $\sim$ 5-10 years) and susequently modified by waves and tides (mesotidal; 2 m - 4m range).

Note: A related delta classification was recently proposed by Lin and Bhattacharya (2021), "Storm-flood-dominated delta: A new type of delta in stormy oceans" which helps formalize the "flood-dominated delta" noted above. Their identification criteria include extensive sharp-based planar to hummocky cross-stratified sandstone beds, commonly presenting as large-sized gutter casts. The gutter casts are interpreted as storm channels formed by erosion resulting from offshore-oriented downwelling currents that may include localized rip currents. In conjunction with these gradient (coastal setup) flows, density (hyperpycnal/hypopycnal) flows may form from sediment-laden floodwaters yielding an efficient offshore sediment transport. Whereas gutters and shallow channels may be important to their model, gutters/channels are not distinctive as these occur in many environments (e.g., Amos at al., 2005). In any case, they propose a four-component pyramidal classification scheme of deltaic deposition to highlight storms as a distinct process and which can be "readily applied to interpret storm-dominated environments and provide new insights into depositional processes of the marine realm."

Figure 28. Flood-dominated deltas with tidal and wave-influence – Gulf of Carpenteria, N. Australia. The Nicholson, Albert and Leinhardt River deltas coalesce in a complex delta plain with many point and some mid-channel bars; numerous tidal creeks, separate and attached to main drainages and a sandy strandline downcurrent. Episodic flood events (large events = cyclones plus monsoons) on small flashy drainages transport large volumes of sediment to the coast.

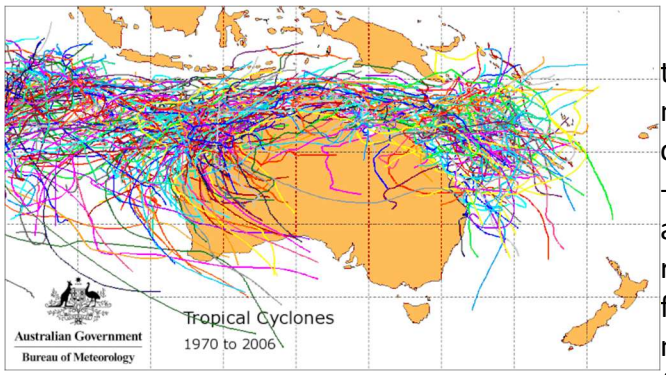

Figure 29.- 35 year track record of Australian tropical cyclones (roughly 10/year; average may be increasing). Per Fielding (2005), a cyclone influences the Burkedin delta every 1 -2 years producing major flooding. Keen et al. (2006; 2012) estimate hurricane recurrence in the Gulf of Mexico at 10 years for event bed deposition and 50 years for major hurricanes depositing thick event beds (e.g., Katrina produced a 0.5 m event bed that thinned to 0.1 m over a distance of 200 K; comparable to thicker storm beds in the geologic record).

Caprock

The caprock is about 15 to 75 cm in thickness, composed largely of pebbles of variable size and coarse sand, and exhibits both massive fabric and crude cross-bedding. And at outcrop #5, the largest caprock pebbles are > 60 mm (Fig. 8) and instead of 99% vein quartz, the clasts include about 25% exotics: red sandstone, metamorphic clasts, including some more equant shapes and large (pebble size) mud chips (the only mud seen thus far) which appears to be a matrix in

places. Aligned plant debris is also common, aligned normal to shore, a centimeter or two below the top surface. And the top surface is often irregular and displays hummocks and other relief in places.

Storm waves have been attributed to "beheading" large subaqueous dunes at outcrop #7 as well as another incursion, 1- 2 m below the caprock in places. Given the very large HCS present at or just below the cap and the sudden introduction of exotic pebbles and abundant plant matter, it seems likely that the powerful storm(s) that produced the very large-scale HCS also produced the pebbly caprock (it appears that U_o. > 2 m/s would be required to entrain the large pebbles; the HCS/U_o. chart shows a range of 2- 3 m/s for the larger bedforms). And a flood, possibly coincident, most likely transported the large exotic pebbles and plant debris at least locally with two inferred distributary mouths nearby and less robust caprock elsewhere may have been sorted or winnowed in place.

But what accounts for the drastic and rapid change in sedimentation, apparent wave energy, and biological activity on top of the cap (assuming that the trend continued as examination of float nearby and outcrops elsewhere suggests that it did)? The fossiliferous wave-rippled thin-bedded sandstones record the first fossil occurrences in the sequence; molds of *Productella sp., Camarotechcia sp., and Crytospirifer sp.*). And the caprock appears largely undisturbed and a gradual high energy foreshore/shoreface transgression is not in evidence. Evidence points to a change in relative sea level and an eustatic rise would act to reduce stream gradients for transport of coarse sediment. And It seems that sea level was on the rise with episodes of wave ravinement near the top of sequence. Basin subsidence is appealing for possible rapidity but it does not fit the situation as well. Johnson et al. (1986) noted that sea level rise may occur fairly rapidly with mid-oceanic ridge activity or mid-plate thermal uplift while McClung et al. (2013; 2016) tie their T-R cycles in upper Devonian rocks in West Virginia to glacial cycles.

CONCLUSION

The Salamanca "flat-pebble" Conglomerate records intense episodic events such as storms and floods along a late Devonian coastline as well as periodic and predictable processes such as tides and fair weather sedimentation. Depositional environments include a progradational flood-dominated delta, pebble-rich marine strata with HCS (some very coarse-grained and of large-scale), a sub-aqueous large-scale ($\sim$ 5 m) dune field formed by meso-tidal flood tides, and a mixed sand/pebble beach. Much of the sequence records delta progradation by cyclone-driven floods and the generation of large scale, coarse-grained HCS. by storm waves. Sediment transport and redistribution along shore and near-offshore likely occurred mainly by longshore and rip currents from the wave breaker/surf zone to the shoreface. Other sediment transport mechanisms such as downwelling from coastal setup, geostrophic flows, and hyperpycnal flows may carry sorted sediment further offshore. Well-exposed channel deposits near the top of the sequence (which overlie wave-truncated dunes and beach deposits at a similar elevations) suggest an expanding delta until an apparent abrupt rise in relative sea level brought a transgression of shallow marine conditions as recorded by thin-bedded wave-formed strata and an abundant fossil fauna directly overlying a pebbly caprock.

SALAMANCA CONGLOMERATE - ROAD LOG

Meeting Point: Rock City State Forest – Little Rock City Rd. at the DEC sign/State Forest boundary

(two small parking lots; carpool if possible)

Meeting Point Coordinates: 42.225830, -78.710587

Meeting Time: 9:30 AM

Rock City State Forest is off Hungry Hollow Rd. which can be approached from US route-219 or State route-353.

Most outcrops are short hikes on trail or just off the road (longest = outcrop #3, about a mile round trip).

Bring a lunch.

Be prepared for sparse facilities; one porta-loo at road's end/outcrop #7.

Latitude	Longitude	Stop or View Description
42.2280	-78.7092	STOP 1. The "Sentinels" - obvious from the first crest of Little Rock City Rd.; well visited but respect private property. Well-weathered, isolated blocks; interpreted as tidal flats and shoals.
42.2265	-78.7137	STOP 2. The "North Face" - the highest outcrops (+10 m; which includes 4-5 m of marine strata) – shoreface/foreshore/channels
42.2259	-78.7175	STOP 3. NW corner of outcrop belt and points S on the Rim Trail, interpreted as a deltaic channelbelt w/shoreface, mouth bar, channels/point bars.
42.2217	-78.7113	STOP 4. Just east of the first rise (escarpment) on Little Rock City Rd. within RCSF. Some point bars (lateral accretion deposits) and channel fills and large x-beds and capped by beds of very large (> 7m) pebbly hummocky cross-strata (HCS). Interpreted as part of the deltaic sequence with some tidal deposits and storm intrusions.
42.2187	-78.7127	STOP 5. A few 100 meters south of #4, east side of the road, just inside treeline, a series of linear outcrops extend south for 100s of meters. Roughly 2 m exposed, mostly HCS, some wave x-lamination, occ. channels/x-beds; very large and pebbly HCS subjacent to caprock; above cap, a thin-bedded fossiliferous sandstone. Interpreted as intense storms then quiescent shallow

		marine conditions; a distinct change in wave climate perhaps best explained by a relatively rapid change in relative sea level/apparent transgression.
42.2094	-78.7108	STOP 6. East of first campsite/shelter, follow white (NCT) blazes; perhaps the most interesting (confusing?) outcrop area. A large channel complex overlying fine-grained wave-rippled sandstone (delta interpretation) with adjoining cross-strata of all scales.
42.2088	-78.7075	STOP 7. The NCT joins outcrop area #6 with #7 and following it south (white blazes) through Little Rock City provides a representative sampling of large-scale (3-5 m) cross-strata (tidal dune field) followed by HCS (dune beheading by waves), then a smattering of channel deposits (tidal or fluvial), then the caprock (a final leveling by waves).

EPILOGUE

James Hall (1843) poetically summed up these formative geologic processes and the passage of time:

"Here was an ocean supplied with all the materials for forming rocky strata: in its deeper parts were going on the finer depositions, and on its shores were produced the sandy beaches, and the pebbly banks. All, for aught we know, was as bright and beautiful as upon our ocean shores of the present day; the tide ebbed and flowed, its waters ruffled by the gentle breeze, and nature wrought in all her various forms as at the present time, though man was not there to say,

How Beautiful!"

REFERENCES

Allen, J.R.L. ,1970, *Physical Processes of Sedimentation,* Allen and Unwin, London, 248 p.

Allen, J.R.L., 1980, Sand waves; a model of origin and internal structure: Sediment Geol. 26, p. 281–328

Allen, J.R.L., 1982, *Sedimentary Structures: Their Character and Physical Basis, Volumes I & II,* Elsevier, Oxford, 592 p./663 p.

Amos, C.L., Li, M.Z. and Choung, K.S., 1996, Storm-generated, hummocky stratification on the outer-Scotian Shelf, *Geo-Marine Letters*, *16*(2), pp. 85-94.

Ashley, G.M.,1990, Classification of large-scale subaqueous bedforms - a new look at an old problem: Journal of Sedimentary Petrology, 60, p. 160–172.

Attal, M., and Lave, J., 2009, Pebble abrasion during fluvial transport - Experimental results and implications for the evolution of the sediment load along rivers: J. Geophys. Res., 114, F04023.

Baird, G.C. and Lash, G.G., 1990, Devonian strata and paleoenvironments - Chautauqua County region, New York State: New York State Geological Association, 62nd Annual Meeting, Field Trip Guidebook, p. A1-46.

Berner, R. A., 1970, Sedimentary pyrite formation: American Journal of Science, 268, p. 13-23.

Berner, R. A., 1997, Paleoclimate – The rise of plants and their effect on weathering and atmospheric CO_2Science, 276, p. 544–546.

Bishuk, Jr., D., Applebaum, R., and Ebert, J.R., 1991, Storm-dominated shelf and tidally-influenced foreshore sedimentation, Upper Devonian Sonyea Group, Bainbridge to Sidney Center, New York: New York State Geological Association, 63rd Annual Meeting, Oneonta, Field Trip Guidebook, p. 413-462.

Bishuk, Jr., D., Hairabedian, J., and Ebert, J.R. 2003, Coastal Margin Interfluve Paleosols and their Stratigraphic Relationships with Tidally-Influenced Deltaic Deposits in the Sonyea Group (Frasnian) of Northwestern Delaware County, New York: New York State Geological Association, 75th Annual Meeting, Hartwick/Oneonta, Field Trip Guidebook, p. 55-101.

Blakey, R., 2017. North American Paleogeography. (http://deeptimemaps.com/map-room/ ; accessed July 2017)

Boswell, R.M, and Donaldson, A.C., 1988, Depositional architecture of the Upper Devonian Catskill Delta complex: Central Appalachian basin, U.S.A.: *in* McMillan, N.J., Embry, A.F. and Glass, D.J. (eds.), Devonian Of The World, Volume II: Sedimentation, Canadian Society of Petroleum Geologists, p. 65-84.

Bourgeois, J. and Leithold, E.L.,1984, Wave-worked conglomerates - depositional processes and criteria for recognition. In: Sedimentology of gravels and conglomerates. E. H. Koster, and R. J. Steel (eds.). Canadian Society of Petroleum Geologists Memoir, v. 10, p. 331-343.

Boyd, R., Dalrymple, R. and Zaitlin, B.A., 1992, Classification of clastic coastal depositional environments, Sedimentary Geology, 80(3-4), pp. 139-150.

Bradley, W.C.. Fahnestock, R.K., and Rowekamp, E.T., 1972, Coarse sediment transport by flood flows, Knik River, Alaska: Geological Society of America Bulletin, v. 83, p. 1261-1284.

Brenchley, P.J. and Newall,G.,1982, Stom-influenced inner-shelf sand lobes in the Caradoc (Ordovician) of Shropshire, England: Journal of Sedimentary Petrology, 52, 1257-1269.

Bridge, J. S., 2000, The geometry, flow patterns and sedimentary processes of Devonian rivers and coasts, New York and Pennsylvania, USA: *in* Friend, P.F., and Williams, B.P.J., (eds.), New perspectives on the Old Red Sandstone, Geological Society of London, Special Publications 180, p. 61-84.

Bridge, J. S., and Droser, M. L., 1985, Unusual marginal-marine lithofacies from the Upper Devonian Catskill clastic wedge: *in* Woodrow, D.L and Sevon, W.D. (eds.), The Catskill Delta, Geological Society of America special paper 201, p. 163-181.

Bridge, J. S., and Willis, B.J., 1994, Marine transgressions and regressions recorded in Middle Devonian shore-zone deposits of the Catskill clastic wedge: Geological Society of America Bulletin, v. 106, p. 1440-1458.

Bridge, J. S., and Demicco, R.V., 2008, Earth surface processes, landforms and sediment deposits: Cambridge University Press, Cambridge, 815 p.

Campbell, C.V., 1966, Truncated wave-ripple laminae. *Journal of Sedimentary Research*, *36*(3), pp.825-828.

Carll, J.F., 1880, The geology of the oil regions of Warren, Venango , Clarion, and Butler Counties: 2nd Penn. Geol. Survey, Rpt. 13, 58 p.

Chan, M. A., Parry, W. T., and Bowman, J. R., 2000, Diagenetic hematite and manganese oxides and fault-related fluid flow in Jurassic sandstones, Southeastern Utah: *AAPG Bulletin*, *84*(9), p. 1281-1310.

Cheel, R. J., 1991, Grain fabric in hummocky cross-stratified storm beds; genetic implications. *Journal of Sedimentary Research,* 61 (1): 102–110.

Clifton, H.E., 1976, Wave-formed sedimentary structures: A conceptual model, pp. 126-148 *in* Davis, R.A. and Ethington, R.L., 1976, Beach and nearshore sedimentation, Society of Economic Paleontologists
and Mineralogists, Spec.Pub. no. 24.

Clifton, H.E., 2003, Supply, segregation, successions, and significance of shallow marine conglomeratic deposits: *Bulletin of Canadian Petroleum Geology*, *51*(4), pp.370-388.

Clifton, H.E., Hunter, R.E., Phillips, R.L., 1971, Depositional structures and processes in the non-barred high-energy nearshore: *Journal of Sedimentary Research* 1971, 41 (3): 651–670.

Coleman, J.M., Gagliano, S.M., and Webb, J.E., 1964, Minor sedimentary structures in a prograding distributary: Marine Geology, v. 1, p. 240-258.

Craft, J. H. and Bridge, J. S., 1987, Shallow-marine sedimentary processes in the Late Devonian Catskill Sea, New York State: Geological Society of America Bulletin, 98, p. 338-355.

Cummings, D.I., Dumas, S., and Dalrymple, R.W., 2009, Fine-grained versus coarse-grained wave ripples generated experimentally under large-scale oscillatory flow: Journal of Sedimentary Research, v. 79, p. 83–93.

Darwin, G.H., 1883, On the formation of ripple-mark in sand. *Proceedings of the Royal Society of London*, *36*(228-231), pp.18-43.

DeCelles, P.G. and Cavazza, W., 1992, Constraints on the formation of Pliocene hummocky cross-stratification in Calabria (southern Italy) from consideration of hydraulic and dispersive equivalence, grain-flow theory, and suspended-load fallout rate: Journal of Sedimentary Research, 62(4), pp.555-568.

Dennison, J.M., 1985. Catskill Delta shallow marine strata: *in* Woodrow, D.L., and Sevon, W.D., (eds.), *The Catskill Delta: GSA Special Paper 201*, p. 91-106.

Dietrich, W.E., 1982, Settling velocity of natural particles: *Water Resources Research*, *18*(6), pp.1615-1626.

Domokos, G., Jerolmack, D.J., Sipos, A.A., Torok, A., 2014, How river rocks round: Resolving the shape-size paradox. PLoS ONE 9(2): e88657.

Duke, W.L., 1985, Hummocky cross-stratification, tropical hurricanes, and intense winter storms: Sedimentology, 32, p. 167-194.

Duke, W. L. and Prave, A. R., 1991, Storm- and tide-influenced prograding shoreline sequences in the Middle Devonian Mahantango Formation, Pennsylvania, *in* Smith, D. G., Reinson, G. E., Zaitlin, B. A., and, Rahmani, R. A. (eds.), Clastic Tidal Sedimentology, Canadian Society of Petroleum Geologists, Memoirs, 16, p. 349-370.

Engel, A., 1951, Quartz Crystal Deposits of Western Arkansas: US Geological Survey Bulletin 973-E, p. 173-259.

Engelder, T., 1986, The use of joint patterns for understanding the Alleghanian Orogeny in the Upper Devonian Appalachian Basin, Finger Lakes District, New York: New York State Geological Association, 58th Annual Meeting, Field Trip Guidebook, p. 129-144.

Ericksen, M.C., Masson, D.S., Slingerland, R., Swetland, D.W., 1990, Numerical simulation of circulation and sediment transport in the late Devonian Catskill Sea, *in* Cross, T.A. (ed), *Quantitative Dynamic Stratigraphy*. Prentice-Hall, Englewood Cliffs, p. 293-305.

Ettensohn, F.R., 1985, The Catskill Delta complex and the Acadian Orogeny; a model: *in* Woodrow, D.L., and Sevon, W.D., (eds.), *The Catskill Delta: GSA Special Paper 201*, p. 39-49.

Faill, R. T., 1985, The Acadian Orogeny and the Catskill Delta, *in* Woodrow, D.L., and Sevon, W.D., (eds.), *The Catskill Delta: GSA Special Paper 201*, p. 15-37.

Fielding, C.R., Alexander, J. and McDonald, R., 1999, Sedimentary facies from ground-penetrating radar surveys of the modern, upper Burdekin River of north Queensland, Australia: consequences of extreme discharge fluctuations, *in* Fluvial Sedimentology VI (Vol. 28), Oxford, UK: Blackwell Publishing Ltd., pp. 347-362.

Fielding, C.R., Trueman, J.D. and Alexander, J., 2005, Sharp-based, flood-dominated mouth bar sands from the Burdekin River Delta of northeastern Australia: extending the spectrum of mouth-bar facies, geometry, and stacking patterns: *Journal of Sedimentary Research*, *75*(1), pp. 55-66.

Fielding, C.R., Trueman, J.D. and Alexander, J., 2006, Holocene depositional history of the Burdekin River Delta of northeastern Australia: a model for a low-accommodation, highstand delta. Journal of Sedimentary Research, 76(3), pp. 411-428.

Gilbert, G.K., 1899, Ripple-marks and Cross-bedding, GSA Bull. V. 10, pp. 135- 140.

Glenn, L.C., 1902, Carbonic and Devonic formations of southwestern New York: NYS Musuem 56th Annual Report.

Greenwood, B. and Sherman, D.J., 1986, Hummocky cross-stratification in the surf zone: flow parameters and bedding genesis, Sedimentology, 33(1), pp.33-45.

Hack, J. T.,1957, Studies of longitudinal stream profiles in Virginia and Maryland: U.S. Geol. Surv. Prof. Paper, 294-B.

Hall, J., Vanuxem, L., Emmons, E., Mather, W. Williams, 1842-43, *Geology of New York...* Carroll & Cook, Albany.

Harms, J.C., Southard, J.B., and Walker, R.G., 1982, Structures and sequences in clastic rocks: SEPM Short Course No. 9., Society of Economic Paleontologists and Mineralogists, Tulsa, OK.

Ito, M., Ishigaki, A., Nishikawa, T., and Saito, T., 2001, Temporal variation in the wavelength of hummocky cross-stratification: implications for storm intensity through Mesozoic and Cenozoic: Geology, v. 29, p. 87–89.

Jelby, M.E., Grundvåg, S.A., Helland-Hansen, W., Olaussen, S. and Stemmerik, L., 2020,Tempestite facies variability and storm-depositional processes across a wide ramp: Towards a polygenetic model for hummocky cross-stratification, Sedimentology, 67(2), pp.742-781.

Johnson, J.G., Klapper, G., and Sandberg, C.A., 1985, Devonian eustatic fluctuations in Euramerica. Geological Society of America Bulletin, 96(5), pp. 567-587.

Johnson, K.G., and Friedman, G.M., 1969, The Tully clastic correlatives (Upper Devonian) of New York State: A model for recognition of alluvial, dune (?), tidal, nearshore (bar and lagoon), and offshore sedimentary environments in a tectonic delta complex, Journal of Sedimentary Petrology, v. 39, 2, p. 451-485.

Keen, T.R., Furukawa, Y., Bentley, S.J., Slingerland, R.L., Teague, W.J., Dykes, J.D. and Rowley, C.D., 2006, Geological and oceanographic perspectives on event bed formation during Hurricane Katrina. *Geophysical Research Letters*, *33*(23).

Keen, T.R., Slingerland, R.L., Bentley, S.J., Furukawa, Y., Teague, W.J. and Dykes, J.D., 2012, Sediment transport on continental shelves: Storm bed formation and preservation in

heterogeneous sediments, *in*: *Sediments, Morphology and Sedimentary Processes on Continental Shelves*, John Wiley & Sons, Ltd.p. 295-310

Kingsley, C.S., 1984, Dagbreek fan-delta: An alluvial placer to prodelta sequence in the Proterozoic Welkom goldfield, Witwatersrand, South Africa, *in* Koster, E.H., and Steel, R.J., (eds.), Sedimentology of gravels and conglomerates: Canadian Society of Petroleum Geologists Memoir 10, p. 321–330.

Klein, W., 2017, Personal Commications - Dr. Klein and Dr. Lisa Amati kindly fielded questions on fossil plants.

Komar, P.D., 1974, Oscillatory Ripple Marks and the evaluation of ancient wave conditions and environments, Journal of Sedimentary Petrology, v. 44, p. 169-180.

Komar, P.D., 1976, Evaluation of wave-generated longshore current velocities and sand transport rates on beaches, pp, 48-53, *in* Davis, R.A. and Ethington, R.L., 1976, Beach and Nearshore Sedimentation, Society of Economic Paleontologists and Mineralogists, Spec.Pub. no. 24.

Komar, P. D., 1998, *Beach Processes and Sedimentation: 2nd edition*, Prentice-Hall, Upper Saddle River, New Jersey, 544 p.

Komar, P.D. and Li, Z., 1986, Pivoting analyses of the selective entrainment of sediments by shape and size with application to gravel threshold, Sedimentology, 33(3), pp.425-436.

Komar, P.D. and Miller, M.C.,1973, The Threshold of Sediment Movement Under Oscillatory Water Waves: Journal of Sedimentary Research, v. 43, p. 1101-1110.

Komar, P. D., and M. C. Miller, 1974, SEDIMENT THRESHOLD UNDER OSCILLATORY WAVES Proceedings of the 14th Conference on Coastal Engineering (June, 1974), Chapter 44.

Kreisa, R.D., 1981, Storm-generated sedimentary structures in subtidal marine facies with examples from the Middle and Upper Ordovician of southwestern Virginia: Journal of Sedimentary Research, 51(3), pp.823-848.

Krumbein, W.C., 1941, The effects of abrasion on the size, shape and roundness of rock fragments: Journal of Geology 49(5), p. 482–520.

Kuenen, P.H., 1956, Experimental abrasion of pebbles, 2, rolling by current: Journal of Geology 64(4):336–368.

Lamb, M.P.; al., et, 2012, Supplemental material: Origin of giant wave ripples in snowball Earth cap carbonate. Geological Society of America. Journal contribution. https://doi.org/10.1130/2012236

Leckie, D, 1988, Wave-formed, coarse-grained ripples and their relationship to hummocky cross-stratification: Journal of Sedimentary Research, 58, 4, p. 607-622.

Leeder, M.R., 2009, *Sedimentology and sedimentary basins: from turbulence to tectonics*. John Wiley & Sons. 768p.

Leithold, E.L. and Bourgeois, J., 1984, Characteristics of coarse-grained sequences deposited in nearshore, wave-dominated environments—examples from the Miocene of south-west Oregon: *Sedimentology*, *31*(6), pp.749-775.

Lin, W. and Bhattacharya, J.P., 2021, Storm-flood-dominated delta: A new type of delta in stormy oceans, *Sedimentology*, *68*(3), pp. 1109-1136.

McClung, W.S., Cuffey, C.A., Eriksson, K.A. and Terry Jr, D.O., 2016, An incised valley fill and lowstand wedges in the Upper Devonian Foreknobs Formation, central Appalachian Basin: implications for Famennian glacioeustasy: *Palaeogeography, palaeoclimatology, palaeoecology*, *446*, pp.125-143. .

Middleton, G.V., 1977, Sedimentary processes – hydraulic interpretation of primary sedimentary structures, *SEPM Reprint Series*, *3*, 285 p.

Millar, S.W.S. and Nelson, F.E., 2001, Clast fabric in relict periglacial colluvium, Salamanca Re-entrant, southwestern NY, USA: Geogr. Ann., 83 A (3), p, 145-156.

Miller, K.L. and Jerolmack, D., 2021, Controls on the rates and products of particle attrition by bed-load collisions: Earth Surface Dynamics, 9(4), pp.755-770.

Miller, K. L., T. Szabó, D. J. Jerolmack, and G. Domokos, 2014, Quantifying the significance of abrasion and selective transport for downstream fluvial grain size evolution: J. Geophys. Res. Earth Surf., 119, p. 2412-2429.

Miser, H.D., 1943, Quartz veins in the Quachita Mountains of Arkansas and Oklahoma, their relation to structure, metamorphism, and metalliferous deposits: Economic Geology, v. 38, i. 2, p. 91-118.

Missimer, T.M. and Maliva, R.G., 2017, Late Miocene fluvial sediment transport from the southern Appalachian Mountains to southern Florida: An example of an old mountain belt sediment production surge, Sedimentology, p. 1365-1391.

Muller, E.H., 1977, Quaternary Geology of New York, Niagara Sheet*:* NYS Museum & Science Service, Map & Chart Series #28.

Myrow, P., and Southard, J., 1996, Tempestite deposition. Journal of Sedimentary Research, v. 66, no. 5.

Novák-Szabó, T., Sipos, A.Á., Shaw, S., Bertoni, D., Pozzebon, A., Grottoli, E., Sarti, G., Ciavola, P., Domokos, G. and Jerolmack, D.J., 2018, Universal characteristics of particle shape evolution by bed-load chipping: Science Advances, 4(3), p. 4946.

Passchier, S., and Kleinhans, M.G., 2005, Observations of sand waves, megaripples, and hummocks in the Dutch coastal area and their relation to currents and combined flow conditions: J. Geophys. Res., 110, F04S15, doi:10.1029/2004JF000215.

Pelletier, B. R., 1958, Pocono paleocurrents in Pennsylvania and Maryland, Geological Society of America Bulletin, v. 69, p. 1033-1064.

Perillo, M. M., Best, J. L., Yokokawa, M., Sekiguchi, T., Takagawa, T. and Garcia, M. H., 2014, A unified model for bedform development and equilibrium under unidirectional, oscillatory and combined-flows: Sedimentology, 61: p. 2063–2085.

Pettijohn, F.J., 1975, Sedimentary Rocks: 3rd edition, Harper&Row, New York, 628 p.

Prave, A. R., Duke, W. L. and Slattery, W., 1996, A depositional model for storm- and tide-influenced prograding siliciclastic shorelines in the Middle Devonian of the central Appalachian foreland basin: Sedimentology, 43, p. 611-629.

Reesink, A.J.H. and Bridge, J.S., 2007, Influence of superimposed bedforms and flow unsteadiness on formation of cross strata in dunes and unit bars: Sedimentary Geology 202, p. 281–296.

Reesink, A.J.H. and Bridge, J.S., 2009, Influence of bedform superimposition and flow unsteadiness on the formation of cross strata in dunes and unit bars – Part 2, further experiments: Sedimentary Geology, v. 222, p. 274-300.

Reesink, A.J.H., Van den Berg, J.H., Parsons, D.R., Amsler, M.L, Best,, J.L., Hardy, R.J., Orfeo, O, Szupiany R.N., 2015, Extremes in dune preservation: Controls on the completeness of fluvial deposits: *Earth-Science Reviews*, 150, p. 652-665.

Reynaud, J.Y. and Dalrymple, R.W., 2012, Shallow-marine tidal deposits *in* Davis, R.A., Jr. and Dalrymple, R.W., (eds.), *Principles of Tidal Sedimentology*, Springer, p. 335-370.

Ruessink, G., Brinkkemper, J.A. and Kleinhans, M.A., 2015, *Geometry of Wave-Formed Orbital Ripples in Coarse Sand:* Journal of Marine Science and Engineering, v. 3, p.1568-1594.

Scotese, C.R., 2000, Upper Devonian Paleoclimate Map (http://www.scotese.com/ldevclim.htm; accessed July 2017).

Slingerland, R.,1986, Numerical computation of co-oscillating palaeotides in the Catskill epeiric Sea of eastern North America: *Sedimentology*, *33*(4), p. 487-497.

Slingerland, R., and Loule, J. P., 1988, Wind/wave and tidal processes along the Upper Devonian Catskill shoreline in Pennsylvania, U.S.A. *in*: McMillan, N. J., Embrya, A. F., and Glass, D. J. (eds.) *Devonian of the World, Vol. II,* Canadian Society of Petroleum Geologists, Memoirs, 14, p. 125-138.

Smith, G.J., and Jacobi, R.D., 1998, Fault-influenced transgressive incised shoreface model for the Canadaway Group, Catskill Delta Complex: Journal of Sedimentary Research B, v.68, p. 668-683.

Smith, G.J., and Jacobi, R.D., 2001, Tectonic and Eustatic Signals in the Sequence Stratigraphy of the Upper Devonian Canadaway Group, New York State: American Association of Petroleum Geologists Bulletin, v. 85, no. 2, p. 325-357.

Smith, G.J., and Jacobi, R.D., 2006. Depositional and tectonic models for Upper Devonian sandstones in western New York state. Guidebook for the 35th Eastern Section AAPG Meeting and 78th NYSGA Field Trips, p. 54–115.

Sneed, E.D., and Folk, R. L., 1958, Pebbles in the lower Colorado River, Texas, a study in particle morphogenesis: Journal of Geology, 66, p. 114-50.

Southard, J., 2006, - *Introduction to Fluid Motions, Sediment Transport, and Current-Generated Sedimentary Structures,* Massachusetts Institute of Technology: *12.090* - MIT OpenCourseWare, https://ocw.mit.edu.

Southard, J. B., Lambié, J. M., Federico, D. C., Pile, H. T. and Weidman, C. R., 1990, Experiments on bed configurations in fine sands under bidirectional purely oscillatory flow, and the origin of hummocky cross-stratification: Journal of Sedimentary Petrology, 60, 1-17.

Streel, M., Caputo, M. V., Loboziak, S., & Melo, J. H. G., 2000, Late Frasnian–Famennian climates based on palynomorph analyses and the question of the Late Devonian glaciations: *Earth-Science Reviews*, *52*(1), p. 121-173.

Stride A.H.,1982, (ed.) Offshore tidal sands: processes and deposits, Chapman & Hall, London, 222 p.

Terwindt, J. H. J., 1971, Sand waves in the southern bight of the North Sea: Marine Geology, v. 10, 1, p. 51-67.

Terwindt, J. H. J., 2009, Origin and sequences of sedimentary structures in inshore meso-tidal deposits of the North Sea: *Holocene marine sedimentation in the North Sea Basin*, *5*, p. 4-26.

Tesmer, I. H., 1963, Geology of Chautauqua County, New York, Part I - Stratigraphy and Paleontology: N.Y. State Museum Bulletin, v. 391.

Tesmer, I. H., 1975, Geology of Cattaraugus County, New York. Buffalo Society of Natural Sciences Bulletin, 27, 105 p.

Thorne, J. A. and Swift, D. J. P., 1989, The effect of long-term sea-level changes on shelf sedimentation--the concept of sediment regime: Kansas Geological Survey, Subsurface Geology, 12, p. 19

Tonnon P.K., van Rijn L.C., Walstra D.J.R., 2007, The morphodynamic modelling of tidal sand waves on the shoreface: Coastal Engineering, 54, 4, p. 279-296.

van Cappelle, M., Stukins, S., Hampson, G. J. and Johnson, H. D., 2016, Fluvial to tidal transition in proximal, mixed tide-influenced and wave-influenced deltaic deposits: Cretaceous lower Sego Sandstone, Utah, USA: Sedimentology, 63, p. 1333–1361.

Walker, R.G., Duke, W.L. and Leckie, D.A., 1983, Hummocky stratification: Significance of its variable bedding sequences: Discussion and reply: Discussion. *Geological Society of America Bulletin*, *94*(10), pp.1245-1249.

Wang, P., 2012, Principles of sediment transport applicable in tidal environments, Chp. 2 *in* Davis, R.A., Jr. and Dalrymple, R.W. (eds.), *Principles of Tidal Sedimentology*, Springer. New York, 621 p.

Willis, B.J. and Bridge, J. S., 1988, Evolution of Catskill River systems, New York State, *in*: McMillan, N. J., Embry, A.F. and Glass, D.J. (eds.), Devonian of the World, Vol. II., Canadian Society of Petroleum Geologists, Memoirs, 14, p. 85-106.

Williams, J.J., Bell, P.S. and Thorne, P.D., 2005, Unifying large and small wave-generated ripples: Journal of Geophysical Research: Oceans, 110(C2), p. 1-18.

Witzke, B.J., 1990, Palaeoclimate constraints for Palaeozoic palaeolatitudes of Laurentia and Euramerica *in* McKerrow, W.S., and Scotese, C.R., (eds.), *Palaeozoic Palaeogeography and Biogeography*:
Geological Society of London Memoir 12, p. 57-73.

Woodrow, D. L., 1985, Paleogeography, paleoclimate, and sedimentary processes of the Late Devonian
Catskill Delta, *in* Woodrow, D.L., and Sevon, W.D., (eds.), *The Catskill Delta: GSA Special Paper 201*, p. 51-63.

Wu, W. and Wang, S.S., 2006, Formulas for sediment porosity and settling velocity: *Journal of Hydraulic Engineering*, *132*(8), pp.858-862.

Zambito, J.J., 2011, The Late Middle Devonian (Givetian) Global Taghanic Biocrisis in its Type Region (Northern Basin): Geologically Rapid Faunal Transitions Driven by Global and Local Environmental Changes: Ph.D, Dissertation, University of Cincinnati, 231 p.